AN-508
Application Note

APPLICATIONS OF PHOTOTRANSISTORS IN ELECTRO-OPTIC SYSTEMS

Prepared by
John Bliss
Applications Engineering

This note reviews phototransistor theory, characteristics and terminology, then discusses the design of electro-optic systems using device information and geometric considerations. It also includes several circuit designs that are suited to dc, low-frequency and high-frequency applications.

MOTOROLA *Semiconductor Products Inc.*

APPLICATIONS OF PHOTOTRANSISTORS IN ELECTRO-OPTIC SYSTEMS

INTRODUCTION

A phototransistor is a device for controlling current flow with light. Basically, any transistor will function as a phototransistor if the chip is exposed to light, however, certain design techniques are used to optimize the effect in a phototransistor.

Just as phototransistors call for special design techniques, so do the circuits that use them. The circuit designer must supplement his conventional circuit knowledge with the terminology and relationships of optics and radiant energy. This note presents the information necessary to supplement that knowledge. It contains a short review of phototransistor theory and characteristics, followed by a detailed discussion of the subjects of irradiance, illuminance, and optics and their significance to phototransistors. A distinction is made between low-frequency/steady-state design and high-frequency design. The use of the design information is then demonstrated with a series of typical electro-optic systems.

PHOTOTRANSISTOR THEORY[1]

Phototransistor operation is a result of the photo-effect in solids, or more specifically, in semiconductors. Light of a proper wavelength will generate hole-electron pairs within the transistor, and an applied voltage will cause these carriers to move, thus causing a current to flow. The intensity of the applied light will determine the number of carrier pairs generated, and thus the magnitude of the resultant current flow.

In a phototransistor the actual carrier generation takes place in the vicinity of the collector-base junction. As shown in Figure 1 for an NPN device, the photo-generated holes will gather in the base. In particular, a hole generated in the base will remain there, while a hole generated in the collector will be drawn into the base by the strong field at the junction. The same process will result in electrons tending to accumulate in the collector. Charge will not really accumulate however, and will try to evenly distribute throughout the bulk regions. Consequently, holes will diffuse across the base region in the direction of the emitter junction. When they reach the junction they will be injected into the emitter. This in turn will cause the emitter to inject electrons into the base. Since the emitter injection efficiency is much larger than the base injection effeciency, each injected hole will result in many injected electrons.

It is at this point that normal transistor action will occur. The emitter injected electrons will travel across the base and be drawn into the collector. There, they will combine with the photo-induced electrons in the collector to appear as the terminal collector current.

Since the actual photogeneration of carriers occurs in the collector base region, the larger the area of this region, the more carriers are generated, thus, as Figure 2 shows, the transistor is so designed to offer a large area to impinging light.

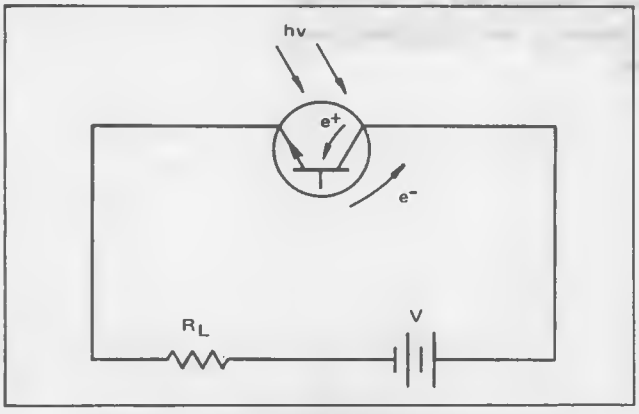

FIGURE 1 – Photo-Generated Carrier Movement in a Phototransistor

[1] For a detailed discussion see Motorola Application Note AN-440, "Theory and Characteristics of Phototransistors."

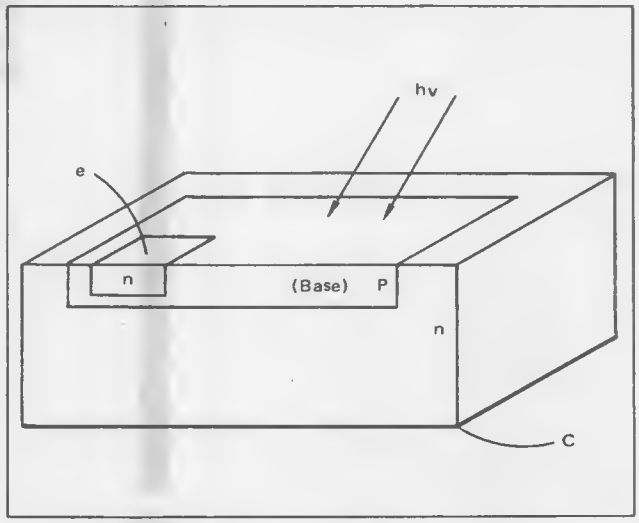

FIGURE 2 – Typical Double-Diffused Phototransistor Structure

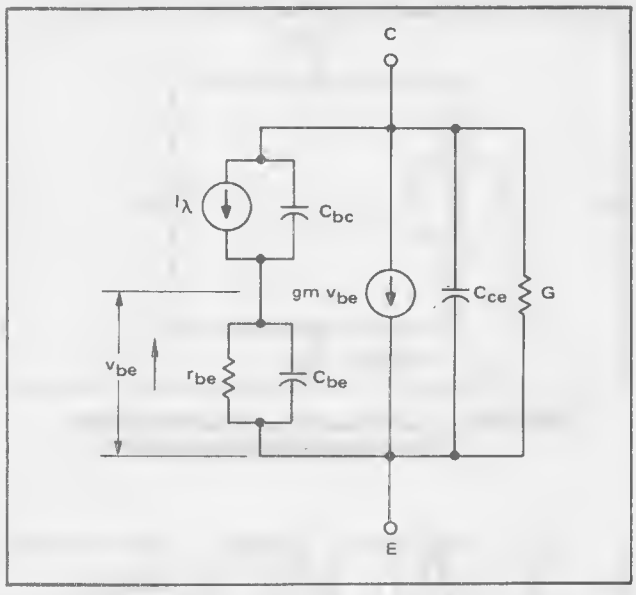

FIGURE 3 – Floating Base Approximate Model of Phototransistor

PHOTOTRANSISTOR STATIC CHARACTERISTICS

A phototransistor can be either a two-lead or a three-lead device. In the three-lead form, the base is made electrically available, and the device may be used as a standard bipolar transistor with or without the additional capability of sensitivity to light. In the two-lead form the base is not electrically available, and the transistor can only be used with light as an input. In most applications, the only drive to the transistor is light, and so the two-lead version is the most prominent.

As a two-lead device, the phototransistor can be modeled as shown in Figure 3. In this circuit, current generator I_λ represents the photo generated current and is approximately given by

$$I_\lambda = \eta F q A \qquad (1)$$

where

η is the quantum efficiency or ratio of current carriers to incident photons,

F is the fraction of incident photons transmitted by the crystal,

q is the electronic charge, and

A is the active area.

The remaining elements should be recognized as the component distribution in the hybrid-pi transistor model. Note that the model of Figure 3 indicates that under dark conditions, I_λ is zero and so v_{be} is zero. This means that the terminal current $I \approx g_m v_{be}$ is also zero.

In reality there is a thermally generated leakage current, I_o, which shunts I_λ. Therefore, the terminal current will be non-zero. This current, I_{CEO}, is typically on the order of 10 nA at room temperature and may in most cases be neglected.

As a three lead device, the model of Figure 3 need only have a resistance, r_b', connected to the junction of C_{bc} and C_{be}. The other end of this resistance is the base terminal. As mentioned earlier, the three lead phototransistor is less common than the two lead version. The only advantages of having the base lead available are to stabilize the device operation for significant temperature excersions, or to use the base for unique circuit purposes.

Mention is often made of the ability to optimize a phototransistor's sensitivity by using the base. The idea is that the device can be electrically biased to a collector current at which h_{FE} is maximum. However, the introduction of any impedance into the base results in a net decrease in photo sensitivity. This is similar to the effect noticed when I_{CEO} is measured for a transistor and found to be greater than I_{CER}. The base-emitter resistor shunts some current around the base-emitter junction, and the shunted current is never multiplied by h_{FE}.

Now when the phototransistor is biased to peak h_{FE}, the magnitude of base impedance is low enough to shunt an appreciable amount of photo current around the base-emitter. The result is actually a lower device sensitivity than found in the open base mode.

Spectral Response – As mentioned previously, a transistor is sensitive to light of a proper wavelength. Actually, response is found for a range of wavelengths. Figure 4 shows the normalized response for a typical phototransistor series (Motorola MRD devices) and indicates that peak response occurs at a wavelength of 0.8 μm. The warping in the response curve in the vicinity of 0.6 μm results from adjoining bands of constructive and destructive interference in the SiO_2 layer covering the transistor surface.

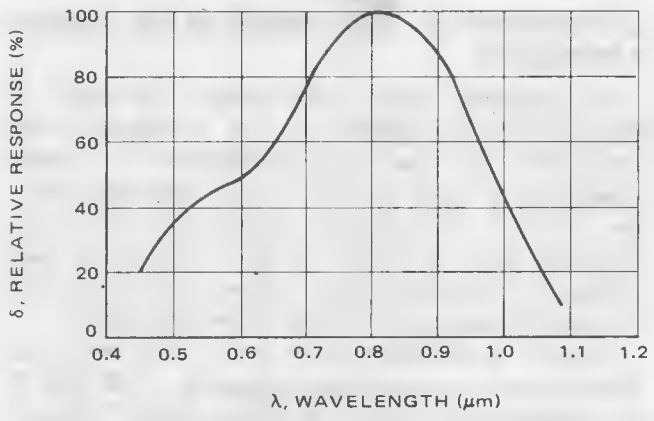

FIGURE 4 – Constant Energy Spectral Response for MRD Phototransistor Series

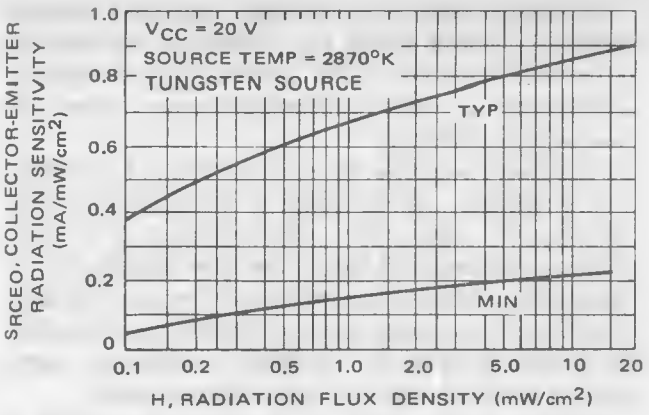

FIGURE 5 — Radiation Sensitivity for MRD450

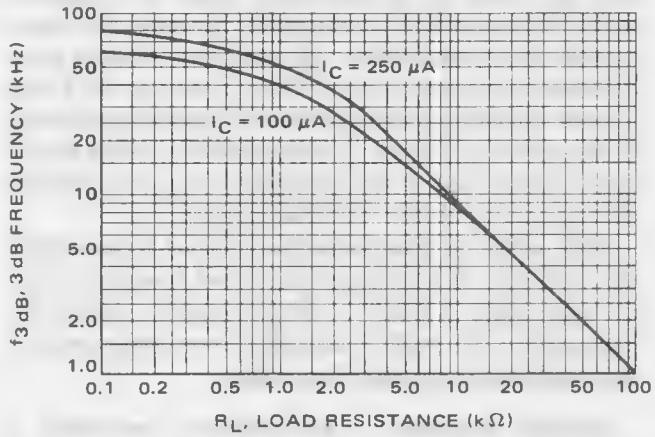

FIGURE 7 — 3 dB Frequency versus Load Resistance for MRD Phototransistor Series

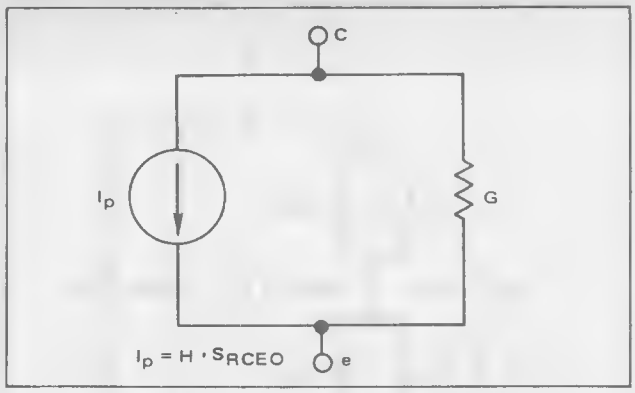

FIGURE 6 — Low-Frequency and Steady-State Model for Floating-Base Phototransistor

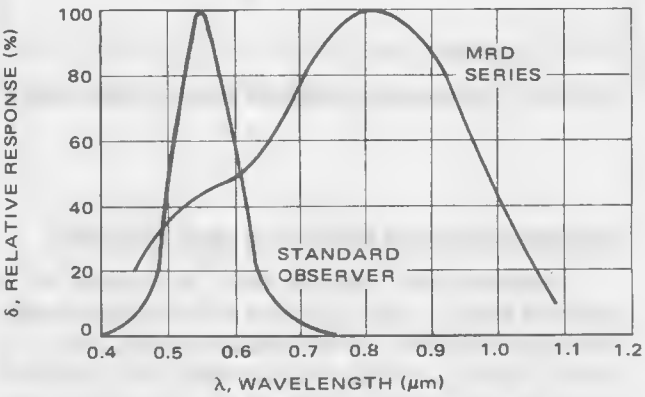

FIGURE 8 — Spectral Response for Standard Observer and MRD Series

Radiation Sensitivity — The absolute response of the MRD450 phototransistor to impinging radiation is shown in Figure 5. This response is standardized to a tungsten source operating at a color temperature of 2870°K. As subsequent discussion will show, the transistor sensitivity is quite dependent on the source color temperature.

Additional static characteristics are discussed in detail in AN-440, and will not be repeated here.

LOW-FREQUENCY AND STEADY-STATE DESIGN APPROACHES

For relatively simple circuit designs, the model of Figure 3 can be replaced with that of Figure 6. The justification for eliminating consideration of device capacitance is based on restricting the phototransistor's use to d.c. or low frequency applications. The actual frequency range of validity is also a function of load resistance. For example, Figure 7 shows a plot of the 3 dB response frequency as a function of load resistance.

Assume a modulated light source is to drive the phototransistor at a maximum frequency of 10 kHz. If the resultant photo current is 100 μA, Figure 7 shows a 3-dB frequency of 10 kHz at a load resistance of 8 kilohms. Therefore, in this case, the model of Figure 6 can be used with acceptable results for a load less than 8 kilohms. For larger loads, the hybrid-pi model must be used.

For the remainder of the discussion of low frequency and steady state design, it is assumed that the simplified model of Figure 6 is valid.

RADIATION AND ILLUMINATION SOURCES

The effect of a radiation source on a photo-transistor is dependent on the transistor spectral response and the spectral distribution of energy from the source. When discussing such energy, two related sets of terminology are available. The first is radiometric which is a physical system; the second is photometric which is a physiological system.

The photometric system defines energy relative to its visual effect. As an example, light from a standard 60 watt-bulb is certainly visible, and as such, has finite photometric quantity, whereas radiant energy from a 60-watt resistor is not visible and has zero photometric quantity. Both items have finite radiometric quantity.

The defining factor for the photometric system is the spectral response curve of a standard observer. This is shown in Figure 8 and is compared with the spectral response of the MRD series. The defining spectral response of the radiometric system can be imagined as unit response for all wavelengths.

A comparison of the terminology for the two systems is given in Table I.

There exists a relationship between the radiometric and photometric quantities such that at a wavelength of 0.55 μm, the wavelength of peak response for a standard observer, one watt of radiant flux is equal to 680 lumens of luminious flux. For a broadband of radiant flux, the visually effective, or photometric flux is given by:

$$F = K \int P(\lambda)\,\delta(\lambda)\,d\lambda \qquad (2a)$$

where

K is the proportionality constant (of 680 lumens/-watt),

P (λ) is the absolute spectral distribution of radiant flux,

$\delta(\lambda)$ is the relative response of the standard observer,

and

$d\lambda$ is the differential wavelength,

A similar integral can be used to convert incident radiant flux density, or irradiance, to illuminance:

$$E = K \int H(\lambda)\,\delta(\lambda)\,d\lambda \qquad (2b)$$

In Equation(2b)if H (λ) is given in watts/ cm^2, E will be in lumens/ cm^2. To obtain E in footcandles (lumens/-ft^2), the proportionality constant becomes

$K = 6.3 \times 10^5$ footcandles/mW/cm^2

Fortunately, it is usually not necessary to perform the above integrations. The photometric effect of a radiant source can often be measured directly with a photometer.

Unfortunately, most phototransistors are specified for use with the radiometric system. Therefore, it is often necessary to convert photometric source data, such as the candle power rating of an incandescent lamp to radiometric data. This will be discussed shortly.

GEOMETRIC CONSIDERATIONS

In the design of electro-optic systems, the geometrical relationships are of prime concern. A source will effectively appear as either a point source, or an area source, depending upon the relationship between the size of the source and the distance between the source and the detector.

Point Sources – A point source is defined as one for which the source diameter is less than ten percent of the distance between the source and the detector, or,

$$\alpha < 0.1r, \qquad (3)$$

where

α is the diameter of the source, and

r is the distance between the source and the detector.

Figure 9 depicts a point source radiating uniformly in every direction. If equation (3) is satisfied, the detector area, A_D, can be approximated as a section of the area of a sphere of radius r whose center is the point source.

The solid angle, ω, in steradians[2] subtended by the detector area is

$$\omega = \frac{A_D}{r^2} \qquad (4)$$

Since a sphere has a surface area of $4\pi r^2$, the total solid angle of a sphere is

$$\omega_S = \frac{4\pi r^2}{r^2} = 4\pi \text{ steradians.}$$

Table II lists the design relationships for a point source in terms of both radiometric and photometric quantities.

The above discussion assumes that the photodetector is alligned such that its surface area is tangent to the sphere with the point source at its center. It is entirely possible that the plane of the detector can be inclined from the

TABLE I – Radiometric and Photometric Terminology

Description	Radiometric	Photometric
Total Flux	Radiant Flux, P, in Watts	Luminous Flux, F, in Lumens
Emitted Flux Density at a Source Surface	Radiant Emittance, W, in Watts/cm^2	Luminous Emittance, L, in Lumens/ft^2 (foot-lamberts), or lumens/cm^2 (Lamberts)
Source Intensity (Point Source)	Radiant Intensity, I_r, in Watts/Steradian	Luminous Intensity, I_L, in Lumens/Steradian (Candela)
Source Intensity (Area Source)	Radiance, Br, in (Watts/Steradian) /cm^2	Luminance, B_L, in (Lumens/Steradian) /ft^2 (footlambert)
Flux Density Incident on a Receiver Surface	Irradiance, H, in Watts/cm^2	Illuminance, E, in Lumens/ft^2 (footcandle)

TABLE II – Point Source Relationships

Description	Radiometric	Photometric
Point Source Intensity	I_r, Watts/Steradian	I_L, Lumens/Steradian
Incident Flux Density	H(Irradiance) = $\frac{I_r}{r^2}$, watts/distance^2	E(Illuminance) = $\frac{I_L}{r^2}$, lumens/distance^2
Total Flux Output of Point Source	$P = 4\pi I_r$ Watts	$F = 4\pi I_L$ Lumens

TABLE III – Design Relationships for an Area Source

Description	Radiometric	Photometric
Source Intensity	B_r, Watts/cm^2/steradian	B_L, Lumens/cm^2/steradian
Emitted Flux Density	$W = \pi B_r$, Watts/cm^2	$L = \pi B_L$, Lumens/cm^2
Incident Flux Density	$H = \frac{B_r A_S}{r^2 + (\frac{D}{2})^2}$, Watts/$cm^2$	$E = \frac{B_L A_S}{r^2 + (\frac{D}{2})^2}$, Lumens/$cm^2$

[2] Steradian: The solid equivalent of a radian.

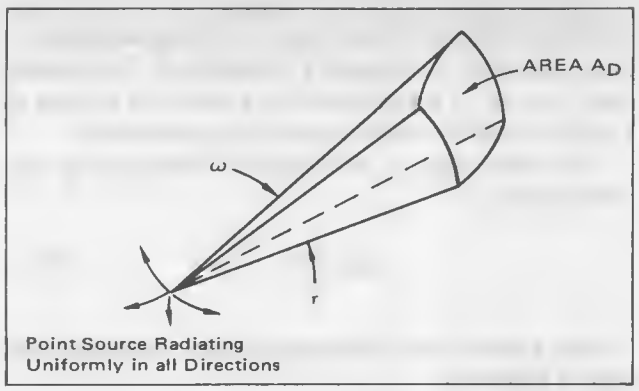

FIGURE 9 – Point Source Geometry

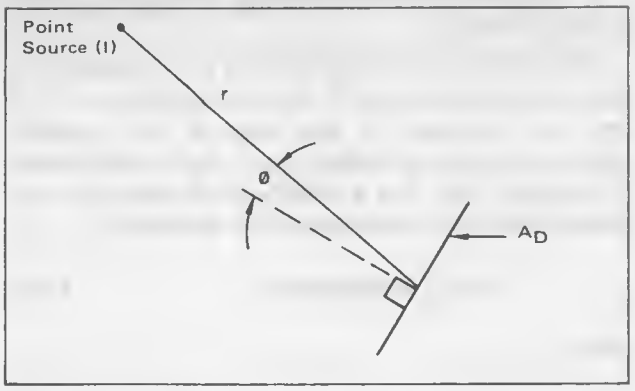

FIGURE 10 – Detector Not Normal to Source Direction

tangent plane. Under this condition, as depicted in Figure 10, the incident flux density is proportional to the cosine of the inclination angle, ϕ. Therefore,

$$H = \frac{I_r}{r^2} \cos \phi, \text{ and} \qquad (5a)$$

$$E = \frac{I_L}{r^2} \cos \phi. \qquad (5b)$$

AREA SOURCES

When the source has a diameter greater than 10 percent of the separation distance,

$$\alpha \geqslant 0.1r, \qquad (6)$$

it is considered to be an area source. This situation is shown in Figure 11. Table III lists the design relationships for an area source.

A special case that deserves some consideration occurs when

$$\frac{\alpha}{2} >> r, \qquad (7)$$

that is, when the detector is quite close to the source. Under this condition,

$$H = \frac{B_r A_S}{r^2 + \left(\frac{\alpha}{2}\right)^2} \approx \frac{B_r A_S}{\left(\frac{\alpha}{2}\right)^2}, \qquad (8)$$

but, the area of the source,

$$A_S = \pi \left(\frac{\alpha}{2}\right)^2, \qquad (9)$$

Therefore,

$$H \approx B_r \pi = W, \qquad (10)$$

That is, the emitted and incident flux densities are equal. Now, if the area of the detector is the same as the area of the source, and equation (7) is satisfied, the total incident energy is approximately the same as the total radiated energy, that is, unity coupling exists between source and detector.

LENS SYSTEMS

A lens can be used with a photodetector to effectively increase the irradiance on the detector. As shown in Figure 12a, the irradiance on a target surface for a point source of intensity, I, is

$$H = I/d^2, \qquad (11)$$

where d is the separation distance.

In Figure 12b a lens has been placed between the source and the detector. It is assumed that the distance d' from the source to the lens is approximately equal to d:

$$d' \approx d, \qquad (12)$$

and the solid angle subtended at the source is sufficiently small to consider the rays striking the lens to be parallel.

If the photodetector is circular in area, and the distance from the lens to the detector is such that the image of the source exactly fills the detector surface area, the radiant flux on the detector (assuming no lens loss) is

$$P_D = P_L = H' \pi r_L^2, \qquad (13)$$

where

P_D is the radiant flux incident on the detector,

P_L is the radiant flux incident on the lens,

H' is the flux density on the lens, and

r_L is the lens radius.

Using equation (12),

$$H' = I/d^2 = H. \qquad (14)$$

The flux density on the detector is

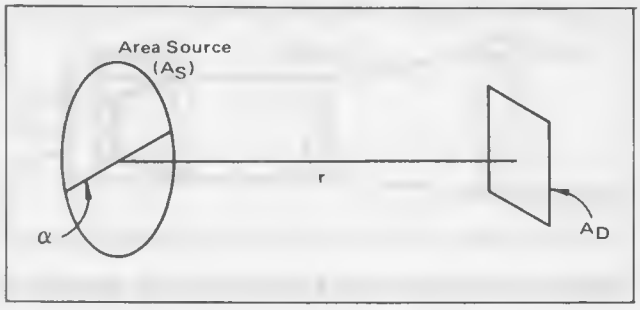

FIGURE 11 – Area Source Geometry

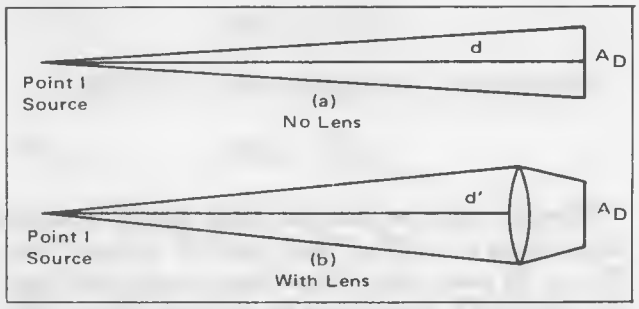

Figure 12 – Use of a Lens to Increase Irradiance on a Detector

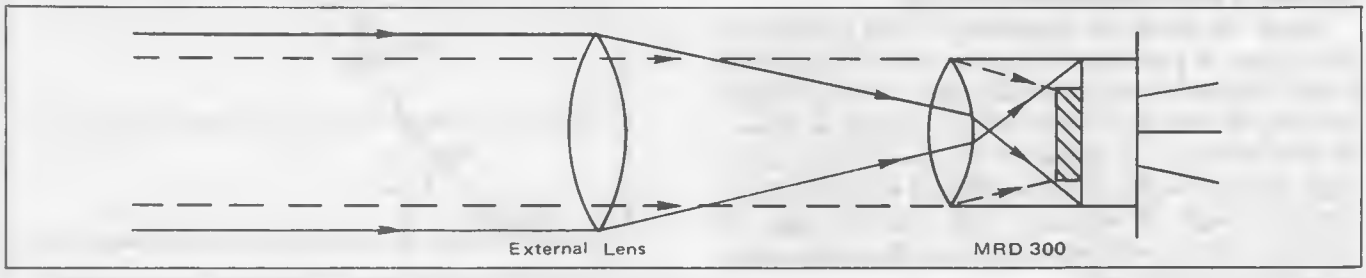

FIGURE 13 – Possible Misalignment Due to Arbitrary Use of
External Lens Dotted Rays Indicate Performance Without External Lens

$$H_D = P_D/A_D, \qquad (15)$$

where A_D is the detector area, given by

$$A_D = \pi r_d^2. \qquad (16)$$

Using (13), (14), and (16) in (15) gives

$$H_D = \frac{1}{d^2}\left(\frac{r_L}{r_d}\right)^2. \qquad (17)$$

Now dividing (17) by (11) gives the ratio of irradiance on the detector with a lens to the irradiance without a lens.

$$\frac{H_D}{H} = \frac{\frac{1}{d^2}\left(\frac{r_L}{r_d}\right)^2}{I/d^2} = \left(\frac{r_L}{r_d}\right)^2. \qquad (18)$$

As (18) shows, if the lens radius is greater than the detector radius, the lens provides an increase in incident irradiance on the detector. To account for losses in the lens, the ratio is reduced by about ten percent.

$$R = 0.9\left(\frac{r_L}{r_d}\right)^2 \qquad (19)$$

where R is the gain of the lens system.

It should be pointed out that arbitrary placement of a lens may be more harmful than helpful. That is, a lens system must be carefully planned to be effective.

For example, the MRD300 phototransistor contains a lens which is effective when the input is in the form of parallel rays (as approximated by a uniformly radiating point source). Now, if a lens is introduced in front of the MRD300 as shown in Figure 13, it will provide a non-parallel ray input to the transistor lens. Thus the net optical circuit will be misaligned. The net irradiance on the phototransistor chip may in fact be less than without the external lens. The circuit of Figure 14 does show an effective system. Lens 1 converges the energy incident on its surface to lens 2 which reconverts this energy into parallel rays. The energy entering the phototransistor lens as parallel rays is the same (neglecting losses) as that entering lens 1. Another way of looking at this is to imagine that the phototransistor surface has been increased to a value equal to the surface area of lens 1.

FIBER OPTICS

Another technique for maximizing the coupling between source and detector is to use a fiber bundle to link the phototransistor to the light source. The operation of fiber optics is based on the principle of total internal reflection.

Figure 15 shows an interface between two materials of different indices of refraction. Assume that the index of refraction, n, of the lower material is greater than that, n', of the upper material. Point P represents a point source of light radiating uniformly in all directions. Some rays from P will be directed at the material interface.

At the interface, Snell's law requires:

$$n \sin\theta = n' \sin\theta', \qquad (20)$$

where

θ is the angle between a ray in the lower material and the normal to the interface,

and

θ' is the angle between a refracted ray and the normal.

Rearranging (20),

$$\sin\theta' = \frac{n}{n'}\sin\theta. \qquad (21)$$

By assumption, n/n' is greater than one, so that

$$\sin\theta' > \sin\theta. \qquad (22)$$

However, since the maximum value of sin θ' is one and occurs when θ' is 90°, θ' will reach 90° before θ does. That is, for some value of θ, defined as the critical angle, θ_C, rays from P do not cross the interface. When $\theta > \theta_C$, the rays are reflected entirely back into the lower material, or total internal reflection occurs.

Figure 16 shows the application of this principle to fiber optics. A glass fiber of refractive index n is clad with a layer of glass of lower refractive index, n'. A ray of light entering the end of the cable will be refracted as shown. If, after refraction, it approaches the glass interface at an angle greater than θ_C, it will be reflected within the fiber. Since the angle of reflection must equal the angle of incidence, the ray will bounce down the fiber and emerge, refracted, at the exit end.

The numerical aperature, NA, of a fiber is defined as the sin of the half angle of acceptance. Application of Snell's law at the interface for θ_C, and again at the fiber end will give

$$NA \equiv \sin\phi = \sqrt{n^2 - n'^2}. \qquad (23)$$

For total internal reflection to occur, a light ray must enter the fiber within the half angle ϕ.

Once a light ray is within the fiber, it will suffer some attenuation. For glass fibers, an absorption rate of from five to ten per cent per foot is typical. There is also an entrance and exit loss at the ends of the fiber which typically result in about a thirty per cent loss.

As an example, an illuminance E at the source end of a three-foot fiber bundle would appear at the detector as

$$E_D = 0.7\,Ee^{-aL} = 0.7\,Ee^{-(0.1)(3)} = 0.51\,E, \qquad (24)$$

where E is the illuminance at the source end,

E_D is the illuminance at the detector end,

a is the absorption rate, and

L is the length.

This assumes an absorption loss of ten percent per foot.

TUNGSTEN LAMPS

Tungsten lamps are often used as radiation sources for photodetectors. The radiant energy of these lamps is distributed over a broad band of wavelengths. Since the eye and the phototransistor exhibit different wavelength-dependent response characteristics, the effect of a tungsten lamp will be different for both. The spectral output of a tungsten lamp is very much a function of color temperature.

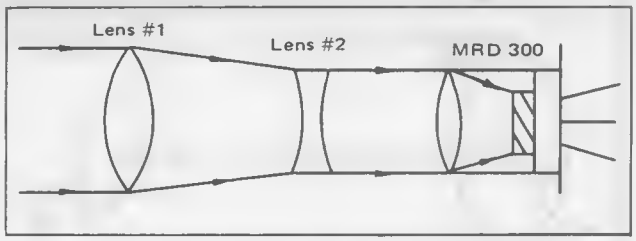

FIGURE 14 – Effective Use of External Optics with the MRD 300

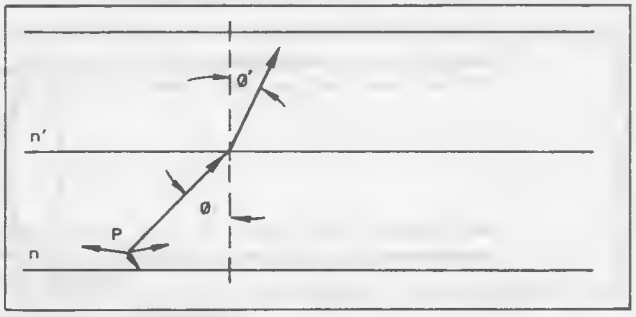

FIGURE 15 – Ray Refraction at an Interface

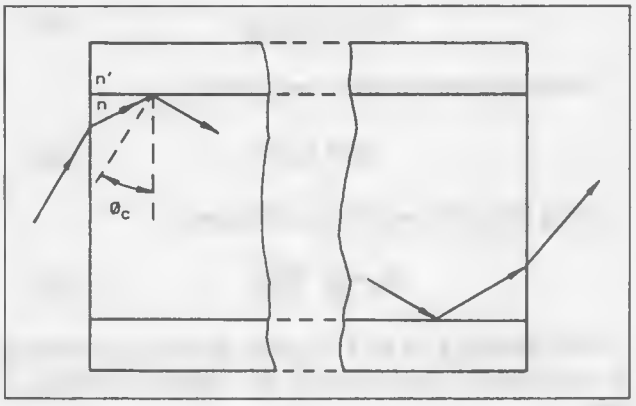

FIGURE 16 – Refraction in an Optical Fiber

Color temperature of a lamp is the temperature required by an ideal blackbody radiator to produce the same visual effect as the lamp. At low color temperatures, a tungsten lamp emits very little visible radiation. However, as color temperature is increased, the response shifts toward the visible spectrum. Figure 17 shows the spectral distribution of tungsten lamps as a function of color temperature. The lamps are operated at constant wattage and the response is normalized to the response at 2800°K. For comparison, the spectral response for both the standard observer and the MRD phototransistor series are also plotted. Graphical integration of the product of the standard observer response and the pertinent source distribution from Figure 17 will provide a solution to equations (2a) and (2b).

Effective Irradiance – Although the sensitivity of a photodetector to an illuminant source is frequently provided, the sensitivity to an irradiant source is more common. Thus, it is advisable to carry out design work in

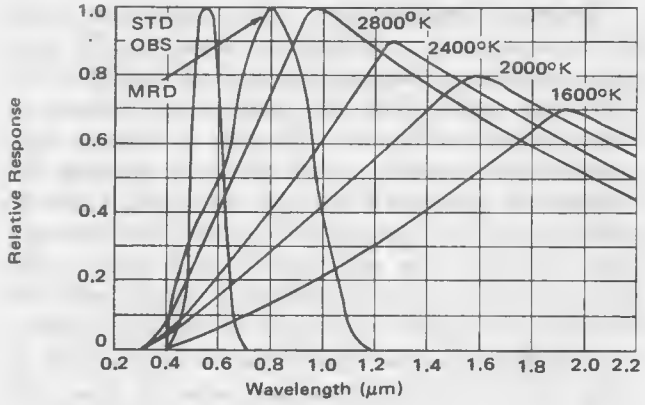

FIGURE 17 – Radiant Spectral Distribution of Tunsten Lamp

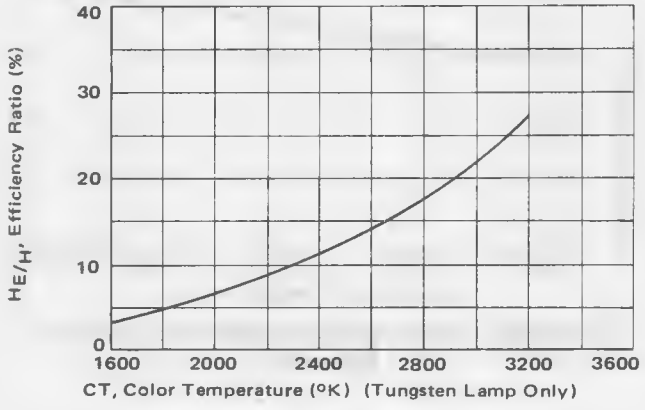

FIGURE 18 – MRD Irradiance Ratio versus Color Temperature

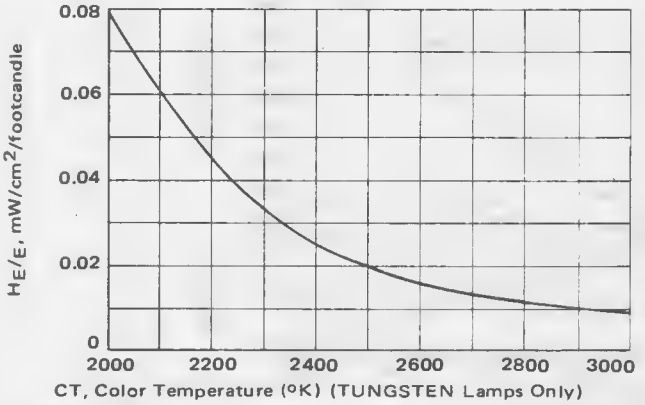

FIGURE 19 – MRD Irradiance/Illuminance Ratio versus Color Temperature

terms of irradiance. However, since the spectral response of a source and a detector are, in general, not the same, a response integration must still be performed. The integral is similar to that for photometric evaluation.

$$P_E = \int P(\lambda)\, Y(\lambda)\, d\lambda \qquad (25)$$

where

P_E is the effective radiant flux on the detector, $P(\lambda)$ is the spectral distribution of source flux

and

$Y(\lambda)$ is the spectral response of the detector.

Again, such an integration is best evaluated graphically. In terms of flux density, the integral is

$$H_E = \int H(\lambda)\, Y(\lambda)\, d\lambda \qquad (26)$$

where H_E is the effective flux density (irradiance) on the detector

and $H(\lambda)$ is the absolute flux density distribution of the source on the detector.

Graphical integration of equations (2b) and (26) has been performed for the MRD series of phototransistors for several values of lamp color temperature. The results are given in Figures 18 and 19 in terms of ratios. Figure 18 provides the irradiance ratio, H_E/H versus color temperature. As the curve shows, a tungsten lamp operating at 2600°K is about 14% effective on the MRD series devices. That is, if the broadband irradiance of such a lamp is measured at the detector and found to be 20 mw/cm², the transistor will effectively see

$$H_E = 0.14\,(20) = 2.8\ \text{mW/cm}^2 \qquad (27)$$

The specifications for the MRD phototransistor series include the correction for effective irradiance. For example, the MRD450 is rated for a typical sensitivity of 0.8 mA/mW/cm². This specification is made with a tungsten source operating at 2870°K and providing an irradiance at the transistor of 5.0 mW/cm². Note that this will result in a current flow of 4.0 mA.

However, from Figure 18, the effective irradiance is

$$H_E = (5.0)(.185) = 0.925\ \text{mW/cm}^2 \qquad (28)$$

By using this value of H_E and the typical sensitivity rating it can be shown that the device sensitivity to a monochromatic irradiance at the MRD450 peak response of 0.8 μm is

$$S = \frac{I_C}{H_E} = \frac{4.0\ \text{mA}}{0.925\ \text{mW/cm}^2} = 4.33\ \text{mA/mW/cm}^2 \qquad (29)$$

Now, as shown previously, an irradiance of 20 mW/cm² at a color temperature of 2600°K looks like monochromatic irradiance at 0.8μm of 2.8 mW/cm² (Equation 27). Therefore, the resultant current flow is

$$I = S\, H_E\, (4.33)(2.8) = 12.2\ \text{mA} \qquad (30)$$

An alternate approach is provided by Figure 20. In this figure, the relative response as a function of color temperature has been plotted. As the curve shows, the response is down to 83% at a color temperature of 2600°K. The specified typical response for the MRD450 at 20mW/cm² for a 2870°K tungsten source is 0.9 mA/mW/cm². The current flow at 2600°K and 20 mW/cm² is therefore

$$I = (0.83)(0.9)(20) = 14.9\ \text{mA} \qquad (31)$$

This value agrees reasonably well with the result obtained in Equation 30. Similarly, Figure 19 will show that a current flow of 6.67 mA will result from an illuminance of 125 foot candles at a color temperature of 2600°K.

Determination of Color Temperature – It is very likely that a circuit designer will not have the capability to measure color temperature. However, with a voltage measuring capability, a reasonable approximation of color temperature may be obtained. Figure 21 shows the classical variation of lamp current, candlepower and lifetime for a tungsten lamp as a function of applied voltage. Figure 22 shows the variation of color temperature as a function of the ratio

$$\rho = \frac{\text{MSCP}}{\text{WATT}} \qquad (32)$$

where

MSCP is the mean spherical candlepower at the lamp operating point and WATT is the lamp IV product at the operating point.

As an example, suppose a type 47 indicator lamp is used as a source for a phototransistor. To extend the lifetime, the lamp is operated at 80% of rated voltage.

Lamp	Rated Volts	Rated Current	MSCP
47	6.3V	150 mA	0.52 approx

Geometric Considerations – The candlepower ratings on most lamps are obtained from measuring the total lamp output in an integrating sphere and dividing by the unit solid angle. Thus the rating is an average, or mean-spherical-candlepower. However, a tungsten lamp cannot radiate uniformly in all directions, therefore, the candlepower varies with the lamp orientation. Figure 23 shows the radiation pattern for a typical frosted tungsten lamp. As shown, the maximum radiation occurs in the horizontal direction for a base-down or base-up lamp. The circular curve simulates the output of a uniform radiator, and contains the same area as the lamp polar plot. It indicates that the lamp horizontal output is about 1.33

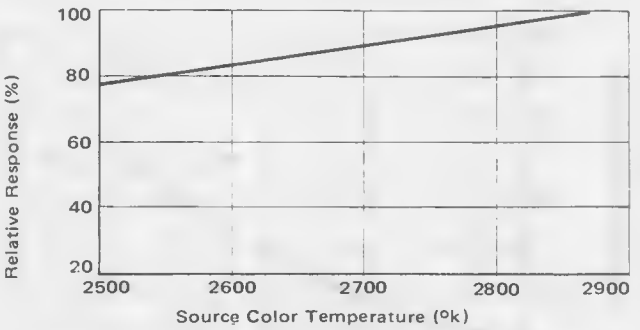

FIGURE 20 – Relative Response of MRD Series versus Color Temperature

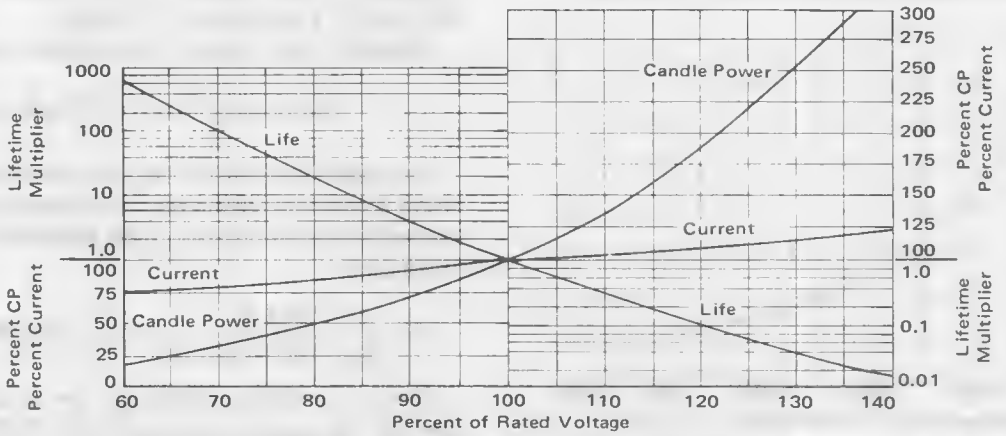

FIGURE 21 – Tungsten Lamp Parameter Variations versus Variations about Rated Voltage

From Figure 21 for 80% rated voltage,

(Rated Current) (Percent current) = (.15)(0.86) = 0.129 ampere

(Rated CP) (Percent CP) = (0.5)(0.52) = 0.26 CP

(Rated Voltage) (Percent Voltage) = (6.3)(0.8) = 5.05 V

$$\text{WATTS} = (5.05)(0.129) = 0.65$$

$$\rho = \frac{0.26}{0.65} = 0.4,$$

From Figure 22, for p = 0.4,

$$\text{CT} = 2300°\text{K},$$

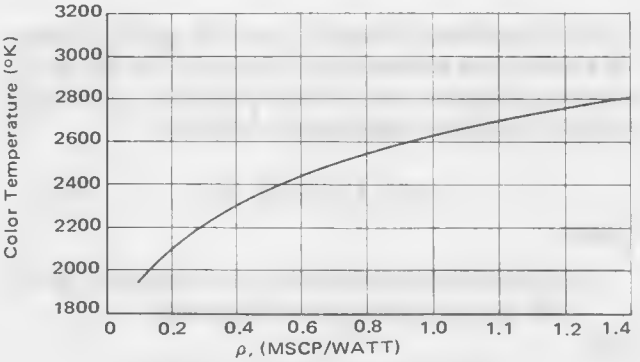

FIGURE 22 – Color Temperature versus Candle Power/Power Ratio

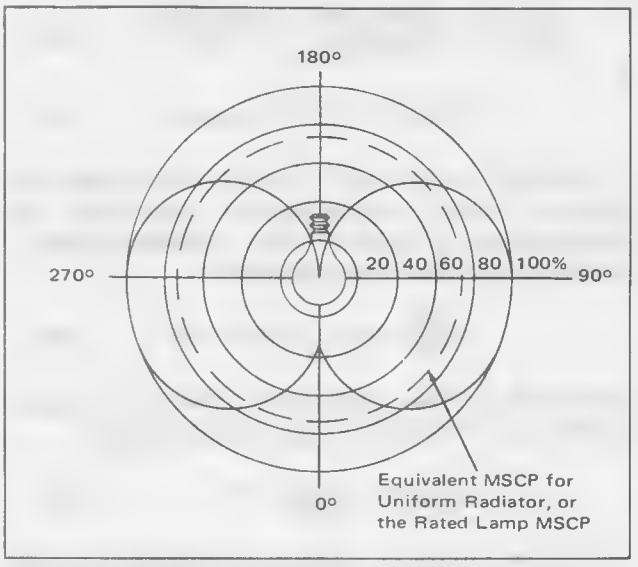

FIGURE 23 – Typical Radiation Pattern for a Frosted Incandescent Lamp

times the rated MSCP, while the vertical output, opposite the base, is 0.48 times the rated MSCP.

The actual polar variation for a lamp will depend on a variety of physical features such as filament shape, size and orientation and the solid angle intercepted by the base with respect to the center of the filament.

If the lamp output is given in horizontal candlepower (HCP), a fairly accurate calculation can be made with regard to illuminance on a receiver.

A third-form of rating is beam candlepower, which is provided for lamps with reflectors.

In all three cases the rating is given in lumens/steradian or candlepower.

SOLID STATE SOURCES

In contrast with the broadband source of radiation of the tungsten lamp, solid state sources provide relatively narrow band energy. The gallium arsenide (GaAs) light-emitting-diode (LED) has spectral characteristics which make it a favorable mate for use with silicon photodetectors. LED's are available for several wavelengths, as shown in Figure 24, but as the figure shows, the GaAs diode and the MRD phototransistor series are particularly compatible. Application of Equation (26) to the GaAs response and the MRD series response indicates that the efficiency ratio, H_E/H, is approximately 0.9 or 90%. That is, an irradiance of 4.0 mW/cm^2 from an LED will appear to the phototransistor as 3.6 mW/cm^2. This means that a typical GaAs LED is about 3.5 times as effective as a tungsten lamp at 2870°K. Therefore, the typical sensitivity for the MRD450 when used with a GaAs LED is approximately

$$S = (0.8)(3.5) = 2.8 \text{ mA/mW/cm}^2. \qquad (33)$$

An additional factor to be considered in using LED's is the polar response. The presence of a lens in the diode package will confine the solid angle of radiation. If the solid angle is θ, the resultant irradiance on a target located at a distance d is

$$H = \frac{4P}{\pi\theta^2 d^2} \text{ watts/cm}^2, \qquad (34)$$

where

P is the total output power of the LED in watts
θ is the beam angle
d is the distance between the LED and the detector in cm.

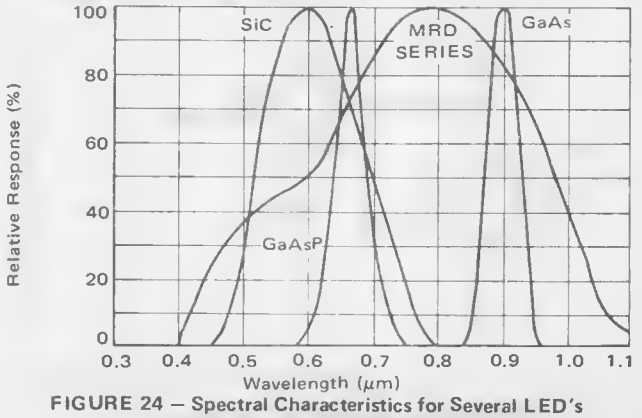

FIGURE 24 – Spectral Characteristics for Several LED's Compared with MRD Series

LOW FREQUENCY AND STEADY STATE APPLICATIONS

Light Operated Relay – Figure 25 shows a circuit in which presence of light causes a relay to operate. The relay used in this circuit draws about 5 mA when Q2 is in saturation Since h_{FE} (min) for the MPS3394 is 55 at a collector current of 2mA, a base current of 0.5 mA is sufficient to ensure saturation. Phototransistor Q1 provides the necessary base drive. If the MRD300 is used, the minimum illumination sensitivity is 4 μA/footcandle, therefore,

$$E = \frac{I_C}{S_{ICEO}} = \frac{0.5 \text{ mA}}{4X10^{-3} \text{ mA/footcandle}} \qquad (35)$$

$$E = 125 \text{ footcandles}$$

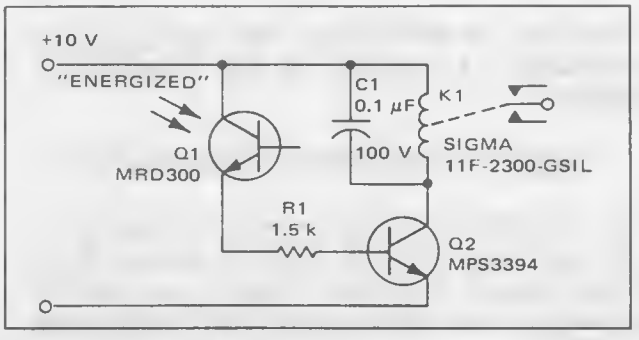

FIGURE 25 – Light-Operated Relay

This light level can be supplied by a flashlight or other equivalent light source.

The equivalent irradiance is obviously that value of irradiance which will cause the same current flow. Assume the light source is a flashlight using a PR2 lamp. The ratings for this lamp are

Lamp	Rated Volts	Rated Current	MSCP
PR2	2.38	0.50 A	0.80

If the flashlight has new batteries the lamp voltage is

$$V_L = 2(1.55) = 3.1 \text{ volts} \qquad (36)$$

This means that the lamp is operated at 130 per cent of rated voltage. From Figure 21 for 130% rated voltage,

(Rated Current) (Percent Current) = (0.5)(1.15) = 0.575 ampere

(Rated CP) (Percent CP) = (0.80)(2.5) = 2 CP

(Rated Voltage) (Percent Voltage) = (2.38)(1.3) = 3.1 volts.

Therefore, the MSCP/watt rating is 1.12. From Figure 22, the color temperature is 2720°K.

Now, from Figure 20, the response at a color temperature of 2720°K is down to 90% of its reference value. At the reference temperature, the minimum S_{RCEO} for the MRD300 is 0.8 mA/mW/cm^2, so at 2720°K it is

$$S_{RCEO\ (MIN)} = (0.9)(0.8) = 0.72 \text{ mA/mW/cm}^2 \qquad (37)$$

and

$$H_E = \frac{I_C}{S_{RCEO}} = \frac{0.5}{0.72} = 0.65 \text{ mW/cm}^2 \qquad (38)$$

However, sensitivity is a function of irradiance, and at 0.695 mW/cm^2 it has a minimum value (at 2720°K) of about 0.45 mA/mW/cm^2, therefore

$$H_E = \frac{0.5}{0.45} = 1.11 \text{ mW/cm}^2 \qquad (39)$$

Again, we note that at an irradiance of 1.11 mW/cm^2, the minimum S_{RCEO} is about 0.54 mA/mW/cm^2. Several applications of the above process eventually result in a convergent answer of

$$H_E \approx 1.0 \text{ mW/cm,}^2 \qquad (40)$$

Now, from the MRD450 data sheet, $S_{RCEO\ (min)}$ at an irradiance of 1.0 mW/cm^2 and color temperature of 2720°K is

$$S_{RCEO} = (0.15)(0.9) = 0.135 \text{ mA/mW/cm}^2 \qquad (41)$$

At 1.0 mW/cm^2, we can expect a minimum I_C of 0.135 mA. This is below the design requirement of 0.5 mA. By looking at the product of $S_{RCEO\ (min)}$ and H on the data sheet curve, the minimum H for 0.5 mA for using the MRD450 can now be calculated.

$$\frac{H}{H_E} = \frac{3.0}{1.0} = \frac{I\ (MRD450)}{I\ (MRD300)} = \frac{I\ (MRD450)}{125} \qquad (42)$$

or

$$I\ (MRD450) = 375 \text{ footcandles} \qquad (43)$$

This value is pretty high for a two D-cell flashlight, but the circuit should perform properly since about 200 footcandles can be expected from a flashlight, giving a resultant current flow of approximately

$$I = \frac{220}{275}(0.5 \text{ mA}) = 0.293 \text{ mA} \qquad (44)$$

This will be the base current of Q2, and since the relay requires 5 mA, the minimum h_{FE} required for Q2 is

$$h_{FE}\ (Q2) = \frac{5}{0.293} = 17. \qquad (45)$$

This is well below the $h_{FE\ (min)}$ specification for the MPS3394 (55) so proper circuit performance can be expected.

A variation of the above circuit is shown in Figure 26. In this circuit, the presence of light deenergizes the relay. The same light levels are applicable. The two relay circuits can be used for a variety of applications such as automatic door activators, object or process counters, and intrusion alarms. Figure 27, for example, shows the circuit of Figure 26 used to activate an SCR in an alarm system. The presence of light keeps the relay deenergized, thus denying trigger current to the SCR gate. When the light is interrupted, the relay energizes, providing the SCR with trigger current. The SCR latches ON, so only a momentary interruption of light is sufficient to cause the alarm to ring continuously. S1 is a momentary contact switch for resetting the system.

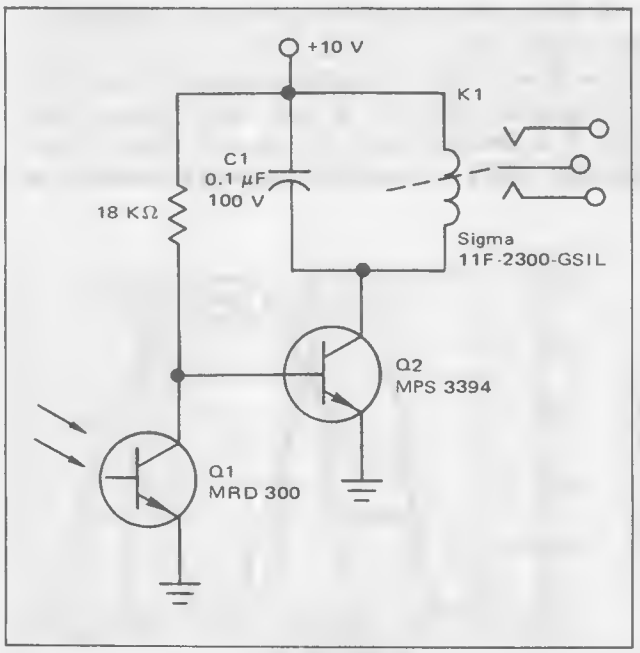

FIGURE 26 — Light De-energized Relay

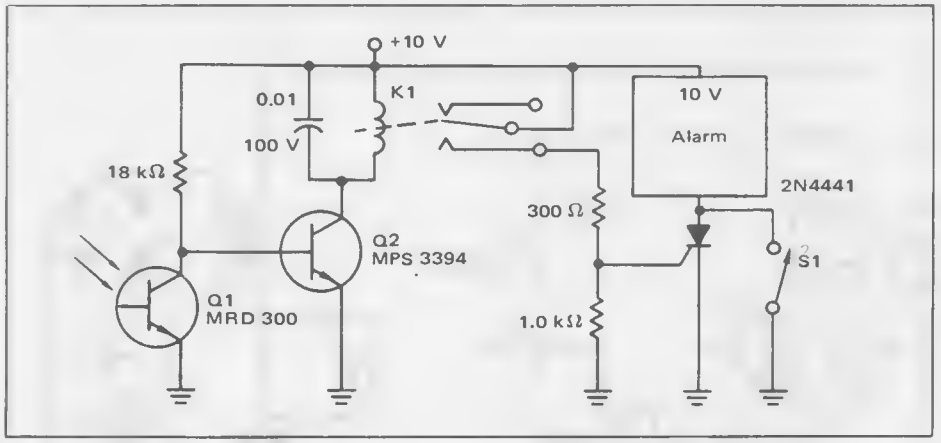

FIGURE 27 – Light-Relay Operated SCR Alarm Circuit

If the SCR has a sensitive gate, the relay can be eliminated as shown in Figure 28. The phototransistor holds the gate low as long as light is present, but pulls the gate up to triggering level when the light is interrupted. Again, a reset switch appears across the SCR.

Voltage Regulator – The light output of an incandescent lamp is very dependent on the RMS voltage applied to it. Since the phototransistor is sensitive to light changes, it can be used to monitor the light output of a lamp, and in a closed-loop system to control the lamp voltage. Such a regulator is particularly useful in a projection system where it is desired to maintain a constant brightness level despite line voltage variations.

Figure 29 shows a voltage regulator for a projection lamp. The RMS voltage on the lamp is set by the firing angle of the SCR. This firing angle in turn is set by the unijunction timing circuit. Transistors Q1 and Q2 form a constant-current source for charging timing capacitor C.

The magnitude of the charging current, the capacitance, C, and the position of R6 set the firing time of the UJT oscillator which in turn sets the firing angle of the SCR. Regulation is accomplished by phototransistor Q3. The brightness of the lamp sets the current level in Q3, which diverts current from the timing capacitor. Potentiometer R6 is set for the desired brightness level.

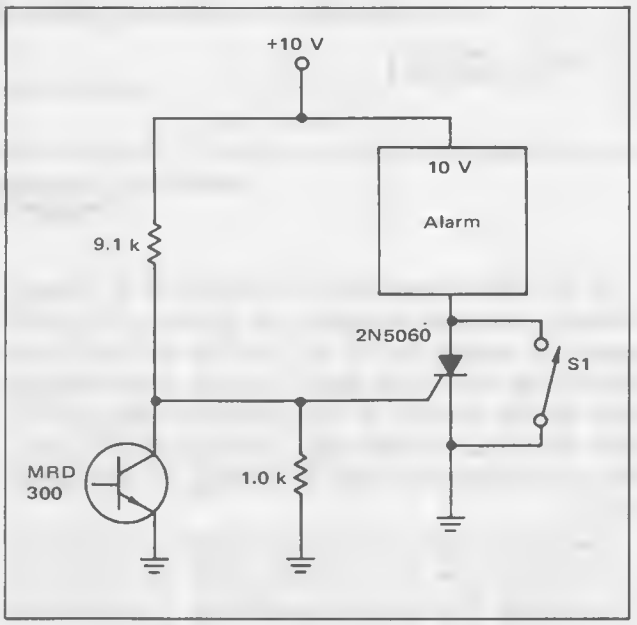

FIGURE 28 – Light Operated SCR Alarm Using Sensitive-Gate SCR

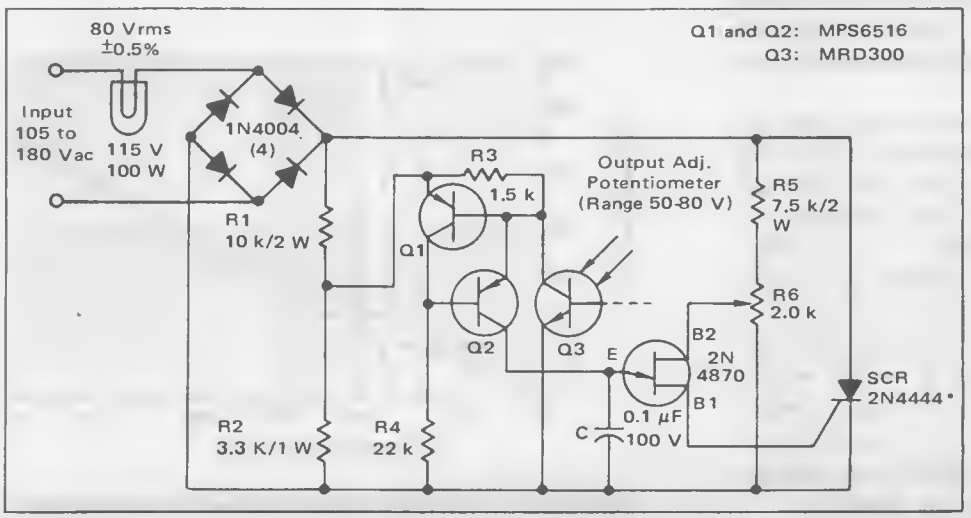

FIGURE 29 – Circuit Diagram of Voltage Regulator for Projection Lamp.

*2N4444 to be used with a heat sink.

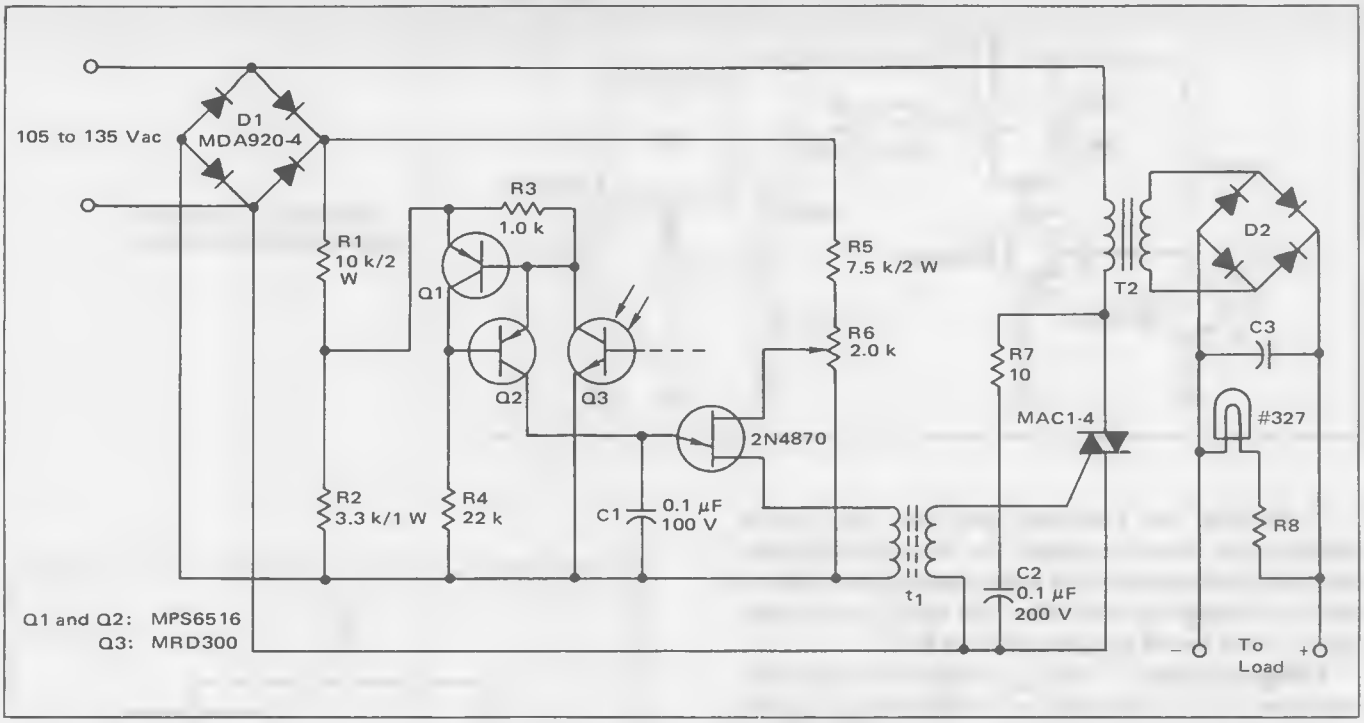

FIGURE 30 – Circuit Diagram of Voltage Regulator for Regulated Power Supply.

If the line voltage rises, the lamp tends to become brighter, causing an increase in the current of Q3. This causes the unijunction to fire later in the cycle, thus reducing the conduction time of the SCR. Since the lamp RMS voltage depends on the conduction angle of the SCR, the increase in line voltage is compensated for by a decrease in conduction angle, maintaining a constant lamp voltage.

Because the projection lamp is so bright, it will saturate the phototransistor if it is directly coupled to it. Either of two coupling techniques are satisfactory. The first is to attenuate the light to the phototransistor with a translucent material with a small iris. The degree of attenuation or translucency must be experimentally determined for the particular projection lamp used.

The second coupling technique is to couple the lamp and phototransistor by a reflected path. The type of reflective surface and path length will again depend on the particular lamp being used.

The voltage regulating scheme can also be used for regulating the output of a high voltage supply. Figure 30 shows the circuit. The basic regulator phase control circuit is similar to that for the projection lamp. However, the unijunction is now coupled to a triac to set the RMS voltage in the primary of power transformer T2. The output of the high-voltage rectifier in the secondary of T2 drives the lamp, therefore, the lamp brightness is dependent on the output voltage. Variations in output voltage cause variations in lamp intensity, thus causing corrective changes in the firing time for the triac. This circuit can be used for very high voltages, and still provide high isolation between the high voltage circuitry and the regulator.

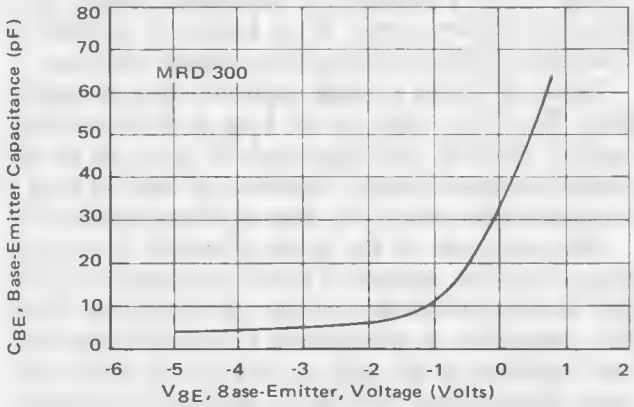

FIGURE 31 – MRD 300 Base-Emitter Junction Capacitance versus Voltage

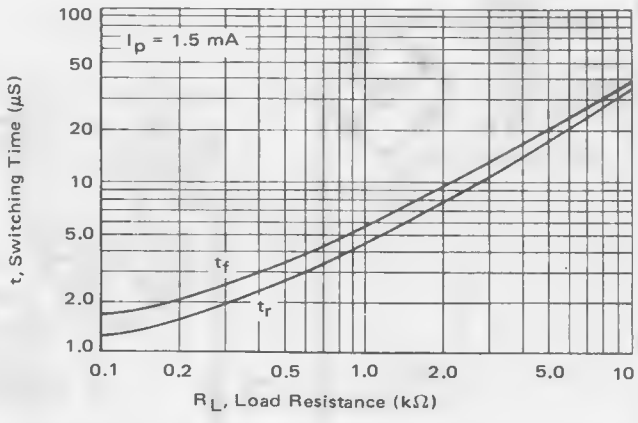

FIGURE 32 – MRD 300 Switching Times versus Load Resistance

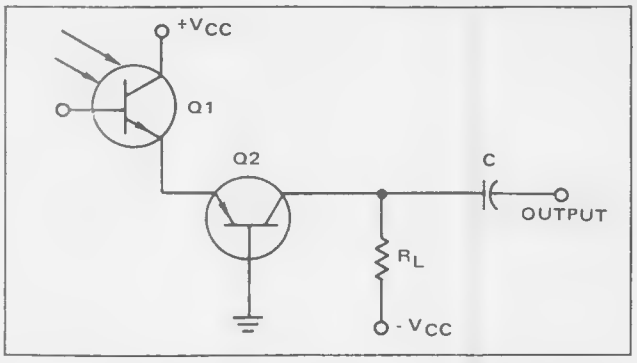

FIGURE 33 – Improved Speed Configuration for Phototransistor

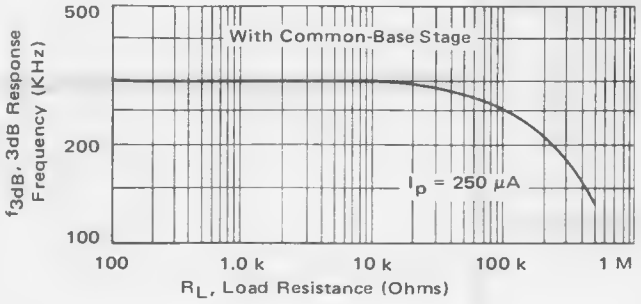

FIGURE 34 – 3dB Frequency Response for Speed-up Circuit

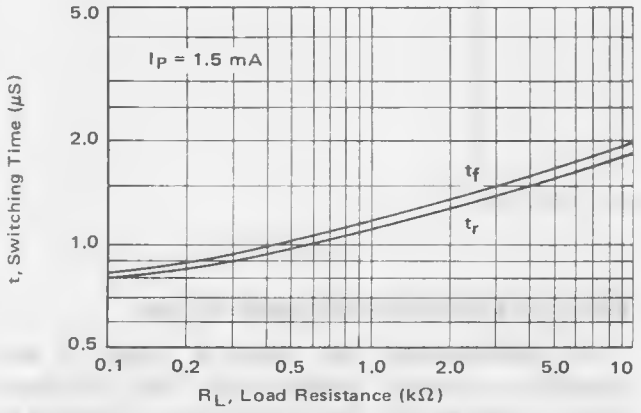

FIGURE 35 – Switching Times with Speed-up Circuit

HIGH FREQUENCY DESIGN APPROACHES

It was shown in Figure 7 that the frequency response of the MRD phototransistor series is quite dependent on the load. Depending on the load value and the frequency of operation, the device can be modled simply as in Figure 6, or else in the modified hybrid-pi form of Figure 3.

While the hybrid-pi model may be useful for detailed analytical work, it does not offer much for the case of simplified design. It is much easier to consider the transistor simply as a current source with a first-order transient response. With the addition of switching characteristics to the device information already available, most design problems can be solved with a minimum of effort.

Switching Characteristics – When the phototransistor changes state from OFF to ON, a significant time delay is associated with the r_{be} C_{be} time constant. As shown in Figure 31, the capacitance of the emitter-base junction is appreciable. Since the device photocurrent is g_m v_{be} (from Figure 3), the load current can change state only as fast as v_{be} can change. Also, v_{be} can change only as fast as C_{be} can charge and discharge through the load resistance. Figure 32 shows the variations in rise and fall time with load resistance. This measurement was made using a GaAs light emitting diode for the light source. The LED output power and the separation distance between the LED and the phototransistor were adjusted for an ON phototransistor current of 1.5 mA. The rise time was also measured for a short-circuited load and found to be about 700 ns.

The major difficulty encountered in high-frequency applications is the load-dependent frequency response. Since the phototransistor is a current source, it is desirable to use a large load resistance to develop maximum output voltage. However, large load resistances limit the useful frequency range. This seems to present the designer with a tradeoff between voltage and speed. However, there is a technique available to eliminate the need for such a tradeoff.

Figure 33 shows a circuit designed to optimize both speed and output voltage. The common-base stage Q2 offers a low-impedance load to the phototransistor, thus maximizing response speed. Since Q2 has near-unity current gain, the load current in R_L is approximately equal to the phototransistor current. Thus the impedance transformation provided by Q2 results in a relatively load-independent frequency response.

The effect of Q2 is shown in Figures 34 and 35. In Figure 34, the 3-dB frequency response as a function of load is shown. Comparing this with Figure 7, the effect of Q2 is quite evident. Comparison of Figures 32 and 35 also demonstrates the effect of Q2.

HIGH FREQUENCY APPLICATIONS

Light-Operated High-Voltage Series Switch – The circuit shown in Figure 36 is a high-voltage switch composed of a series string of SCRs which are triggered simultaneously from a single light source. Triggering is accomplished with phototransistors (MRD300) driven by a xenon flash tube through a fiber-optic bundle.

Across each SCR is a 1.5-MΩ resistor in series with a 51-kΩ resistor. These resistors form not only the voltage equalization network for the series-connected SCRs, but also voltage dividers for each phototransistor, with 20 volts developed across each 0.1-μF capacitor and 51-kΩ resistor. This voltage provides collector bias for each phototransistor and a source of gate current for each SCR. When the xenon tube is flashed, the light is fed into the fiber-optic bundle where it is split into ten outputs of approximately equal amplitude and fed simultaneously to each phototransistor. As each phototransistor conducts, it discharges the 0.1-μF capacitor into the gate of its corresponding SCR via the 510 ohm resistor, turning all

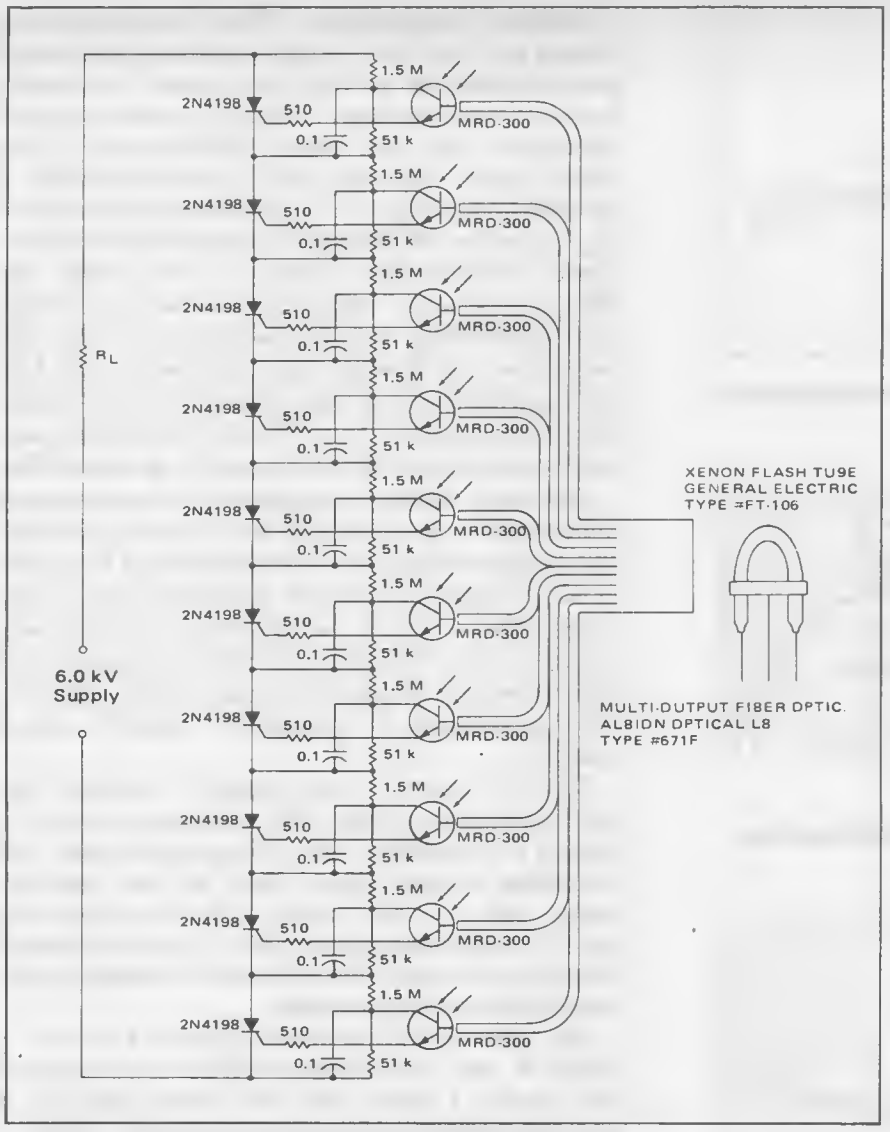

FIGURE 36 – Light-Operated 6 kV Series Switch

the SCR's on at once.

Triggering series-connected SCRs by this method offers several advantages over other types of triggering. The use of light via phototransistors results in simultaneous firing of the SCRs, thus eliminating the inductive delays that would result if conventional wiring were used to transport a gate signal from a central source. Also, the use of fiber optics eliminates the need for special triggering transformers that can withstand the high voltages that would exist between windings.

The turn-on time of the circuit shown was measured to be about 300 ns at 1-A anode current; the maximum capability of the circuit is a 100-A pulse for 4 ms with a 6-kV input voltage. The SCRs must have matched rise times so that the slowest units will not be gated ON by anode breakover due to earlier turn on of the faster devices.

This circuit would be most useful in high-voltage crowbar circuits or high-voltage pulse forming networks.

PHOTOTRANSISTOR INTRUSION ALARM

The light-operated relay circuit in Figure 27 was suggested as a possible intrusion alarm. While this circuit would be sufficient for such an application, it is limited in effectiveness. First, the light beam can be seen, forwarning an intruder, and second, the system is non-selective; that is, any light can override the system. A worst case combination of these faults would enable an intruder to see the alarm system and override it with a flashlight while passing through the beam.

The obvious solution to these problems is to make the beam invisible, and make the system frequency selective.

Making the beam invisible is relatively easy. An incandescent lamp emits a large amount of near-infrared energy, and a silicon phototransistor is most sensitive in the near-infrared region. Inexpensive filters can be used to block all visible light but pass the near-infrared. Thus the beam is invisible.

Making the system frequency selective is a little more involved. On the detector end, the phototransistor can

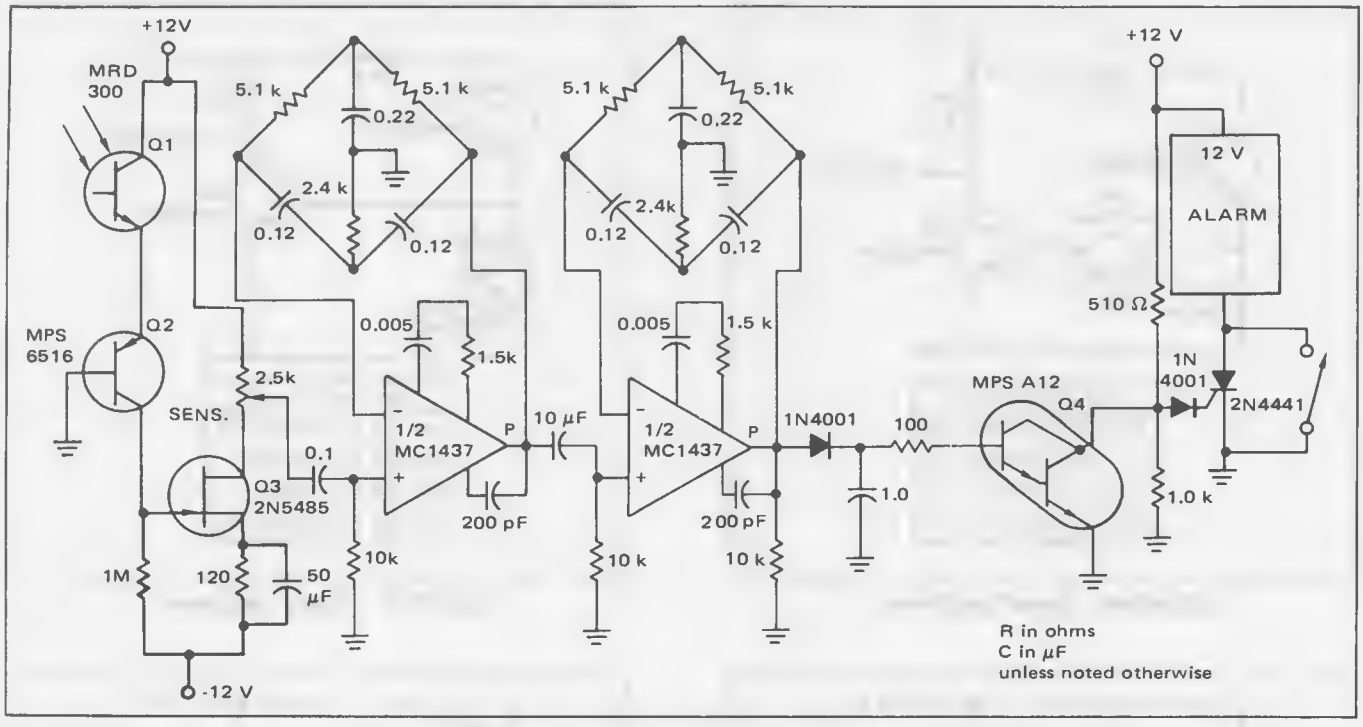

FIGURE 37 – Frequency Selective Photo-alarm

drive a band-pass network. One approach is shown in Figure 37. An MRD300 phototransistor with a common-base speed-up stage drives a FET preamplifier, Q3. The preamp output is fed to a pair of series-connected band-pass amplifiers which use Twin-T feedback networks for frequency selectivity. The filter/amplifier output is fed to a peak detector circuit which holds Q4 in saturation. This deprives the SCR of trigger voltage.

When the input to the phototransistor is interrupted, the SCR is triggered ON and the alarm sounds.

The light source is modulated to match the pass frequency of the receiver. Small lamps (#327 for example) can be electrically modulated up to several hundred hertz. Larger lamps require electro-mechanical chopping to obtain reasonable operating frequencies. Such electro-mechanical chopping can be done with a motor and a punched wheel as shown in Figure 38.

If an intrusion alarm is to be used in the vicinity of line operated background light, the modulation should not be harmonically related to 60 Hz.

A separate source and detector do pose a tricky problem in alignment. However, by mounting both in the same package and using a passive reflector to return the emitted beam to the detector, alignment is greatly simplified.

Remote Strobeflash Slave Adapter – At times when using an electronic strobe flash, it is desirable to use a remote, or "slave" flash synchronized with the master. The circuit in Figure 39 provides the drive needed to trigger a slave unit, and eliminates the necessity for synchronizing wires between the two flash units.

The MRD300 phototransistor used in this circuit is cut

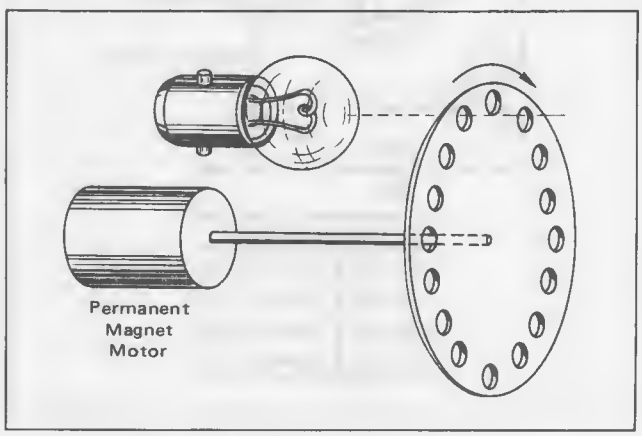

FIGURE 38 – Electro-Mechanical Lamp Modulator

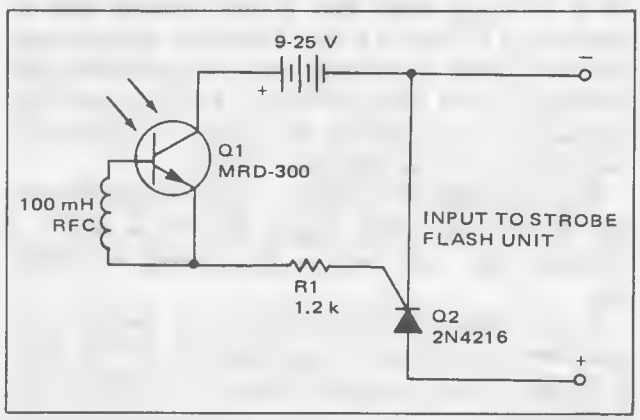

FIGURE 39 – Strobeflash Slave Adapter

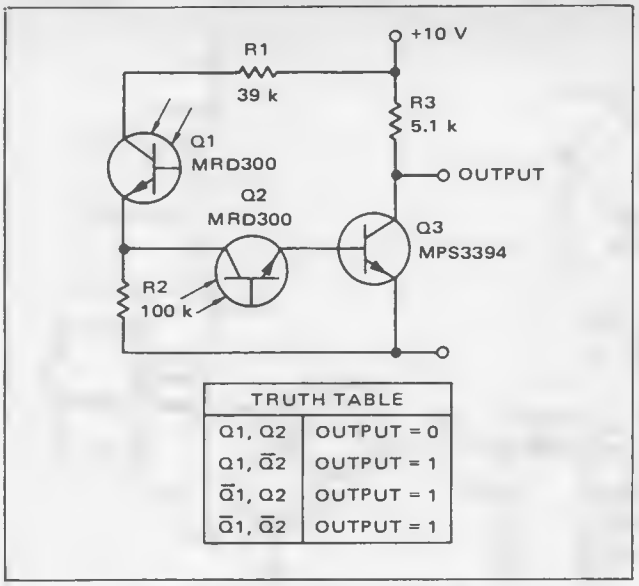

TRUTH TABLE	
Q1, Q2	OUTPUT = 0
Q1, $\overline{Q2}$	OUTPUT = 1
$\overline{Q1}$, Q2	OUTPUT = 1
$\overline{Q1}$, $\overline{Q2}$	OUTPUT = 1

FIGURE 40 – Optical Logic Driver

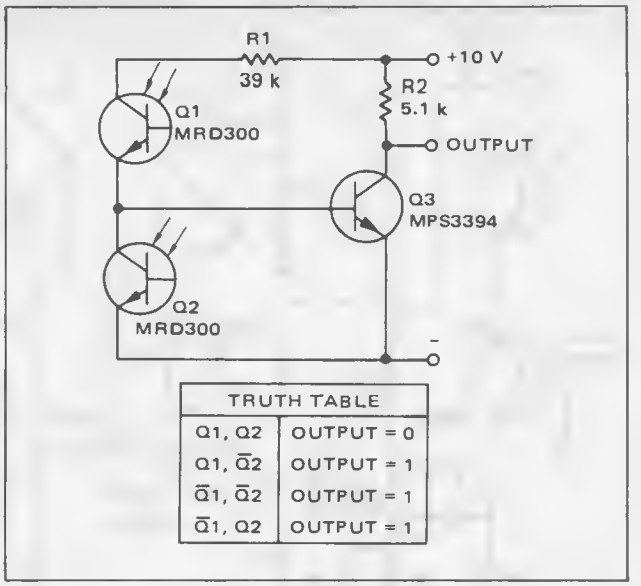

TRUTH TABLE	
Q1, Q2	OUTPUT = 0
Q1, $\overline{Q2}$	OUTPUT = 1
$\overline{Q1}$, $\overline{Q2}$	OUTPUT = 1
$\overline{Q1}$, Q2	OUTPUT = 1

FIGURE 41 – Optical Logic Driver

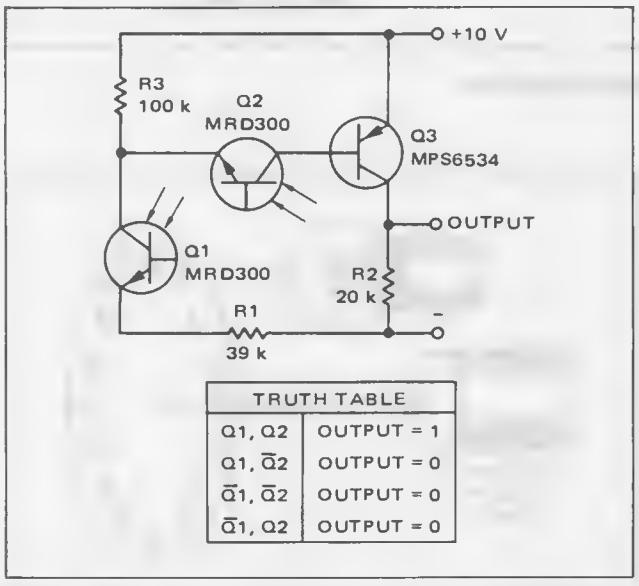

TRUTH TABLE	
Q1, Q2	OUTPUT = 1
Q1, $\overline{Q2}$	OUTPUT = 0
$\overline{Q1}$, $\overline{Q2}$	OUTPUT = 0
$\overline{Q1}$, Q2	OUTPUT = 0

FIGURE 42 – Optical Logic Driver

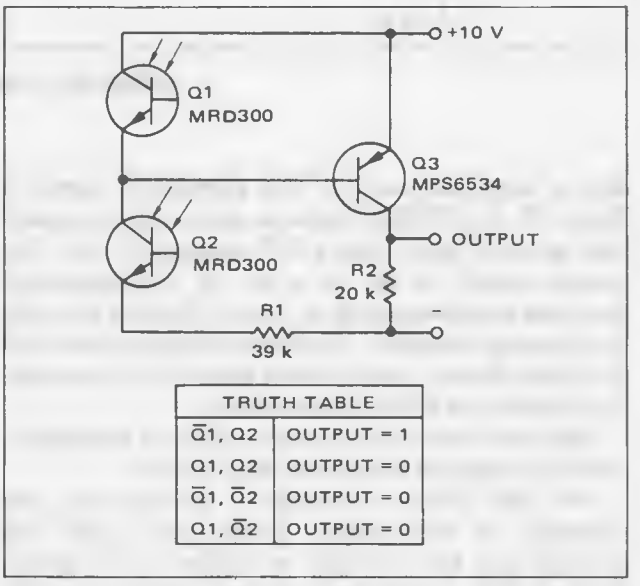

TRUTH TABLE	
$\overline{Q1}$, Q2	OUTPUT = 1
Q1, Q2	OUTPUT = 0
$\overline{Q1}$, $\overline{Q2}$	OUTPUT = 0
Q1, $\overline{Q2}$	OUTPUT = 0

FIGURE 43 – Optical Logic Driver

off in a V_{CER} mode due to the relatively low dc resistance of rf choke L1 even under high ambient light conditions. When a fast-rising pulse of light strikes the base region of this device, however, L1 acts as a very high impedance to the ramp and the transistor is biased into conduction by the incoming pulse of light.

When the MRD300 conducts, a signal is applied to the gate of SCR Q2. This triggers Q2, which acts as a solid-state relay and turns on the attached strobeflash unit.

In tests this unit was unaffected by ambient light conditions. It fired up to approximately 20 feet from strobe-light flashes using only the lens of the MRD300 for light pickup.

Optical Logic Drivers for Power Devices – It is possible to provide logic control of power devices with optical signals if circuits such as those shown in Figures 40 through 43 are used to convert the light signals into electrical signals. The truth tables for these circuits show outputs for positive logic.

For the circuit shown in Figure 40, a "one" output is obtained at all times except when both Q1 and Q2 are exposed to bright light. Approximately 100 foot-candles to Q1 and Q2 will drive Q3 into saturation. Resistor R2 provides a path for leakage currents so that Q3 does not conduct until an adequate light level is presented to Q1 and Q2. The positive output will provide almost 2 mA to a load.

The circuit shown in Figure 41 provides a positive output voltage at all times except when Q1 is on and Q2 is

off. For this case, the base drive to Q3 is provided through R1 and Q1. As in the previous circuit, normal room lighting does not turn Q3 on, but about 100 foot-candles from a flashlight shining on Q1 will allow Q3 to saturate.

The maximum current this circuit can provide a load is 2 mA. The inverse of the output of the two previous circuits can be obtained through the use of an additional inverting stage or by the circuits shown in Figures 42 and 43. If a current sink is required, an inverter should be used, but if a current source is required, the circuits in Figures 42 and 43 should be used. The output of the circuit shown in Figure 42 is zero at all times except when both Q1 and Q2 are on. As in the previous circuits, about 100 foot-candles of illumination on Q1 and Q2 is enough to saturate Q3 so that it can provide at least 10 mA to a load. The value of R2 is high so it does not require any current that can be supplied to the load. A current in R2 of 1/2 mA gives satisfactory results. Resistor R3 provides a path for leakage currents so that Q3 does not conduct until Q1 and Q2 are illuminated.

The circuit in Figure 43 provides a zero output for all conditions except when Q1 is off and Q2 is on. For this condition, base current is provided to Q3 through Q2 and R1. Here also, 100 foot-candles is enough to allow Q3 to saturate and drive a 10 mA load. For this circuit, also, the values of R2 is high so it does not rob current from the load. Q1 must be turned on hard enough to shunt the base-emitter junction of Q3 to keep Q3 from coming on when Q2 is on. This is achieved with the illumination intensity mentioned previously.

The circuits of Figures 40 through 43 might also be used with LED's as sources. This would be useful when it is desired to maintain high isolation between signal and power circuitry.

As stated earlier, the MPS3394 has a minimum h_{FE} of 55 at I_C = 2 mA. It was also pointed out that a base current of 0.5 mA will guarantee saturation of this device. It is, therefore, required that LED's drive both Q1 and Q2 in Figure 4 to provide 0.5 mA photo current. Assume the GaAs LED's are to be used with the following specifications:

Output Power, P, 1.5 mW min at I_D = 100 mA
Beam angle, $\Phi = 20^o$
Spectral Response, as shown in Figure 24

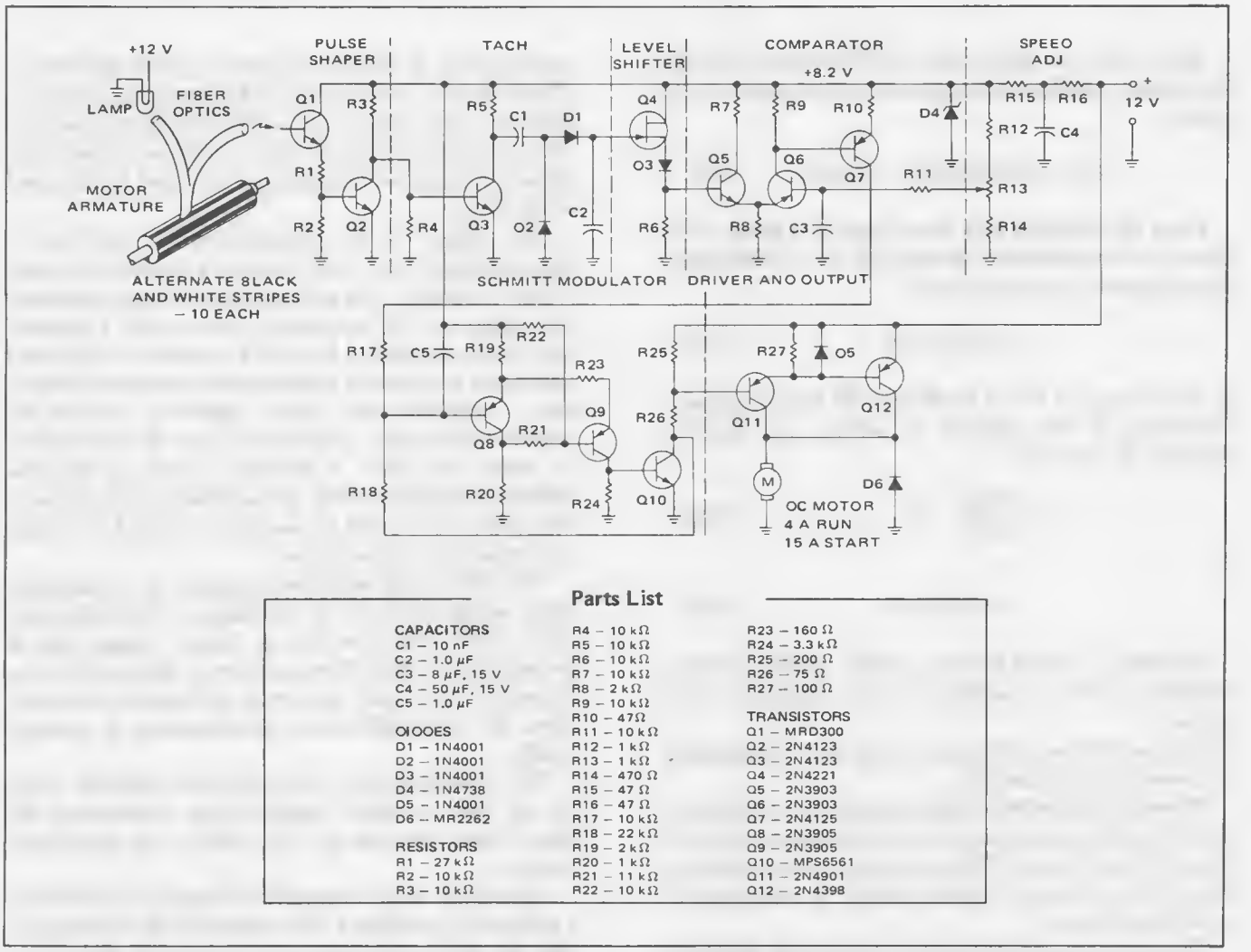

Parts List

CAPACITORS
C1 – 10 nF
C2 – 1.0 μF
C3 – 8 μF, 15 V
C4 – 50 μF, 15 V
C5 – 1.0 μF

DIODES
D1 – 1N4001
D2 – 1N4001
D3 – 1N4001
D4 – 1N4738
D5 – 1N4001
D6 – MR2262

RESISTORS
R1 – 27 kΩ
R2 – 10 kΩ
R3 – 10 kΩ
R4 – 10 kΩ
R5 – 10 kΩ
R6 – 10 kΩ
R7 – 10 kΩ
R8 – 2 kΩ
R9 – 10 kΩ
R10 – 47Ω
R11 – 10 kΩ
R12 – 1 kΩ
R13 – 1 kΩ
R14 – 470 Ω
R15 – 47 Ω
R16 – 47 Ω
R17 – 10 kΩ
R18 – 22 kΩ
R19 – 2 kΩ
R20 – 1 kΩ
R21 – 11 kΩ
R22 – 10 kΩ
R23 – 160 Ω
R24 – 3.3 kΩ
R25 – 200 Ω
R26 – 75 Ω
R27 – 100 Ω

TRANSISTORS
Q1 – MRD300
Q2 – 2N4123
Q3 – 2N4123
Q4 – 2N4221
Q5 – 2N3903
Q6 – 2N3903
Q7 – 2N4125
Q8 – 2N3905
Q9 – 2N3905
Q10 – MPS6561
Q11 – 2N4901
Q12 – 2N4398

FIGURE 44 – Regulated DC Motor Control with Feedback from Optical Pickoff

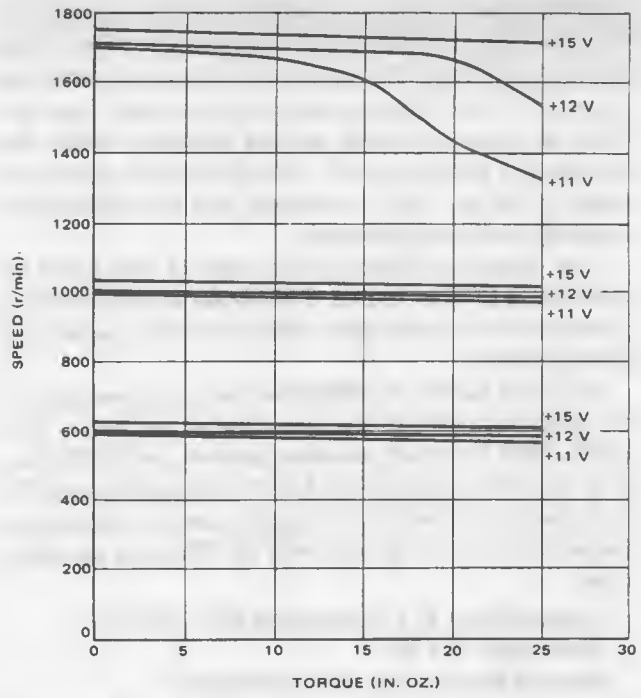

FIGURE 45 – Temperature Characteristics of Motor Controlled by Speed Control Circuit with Optical Feedback

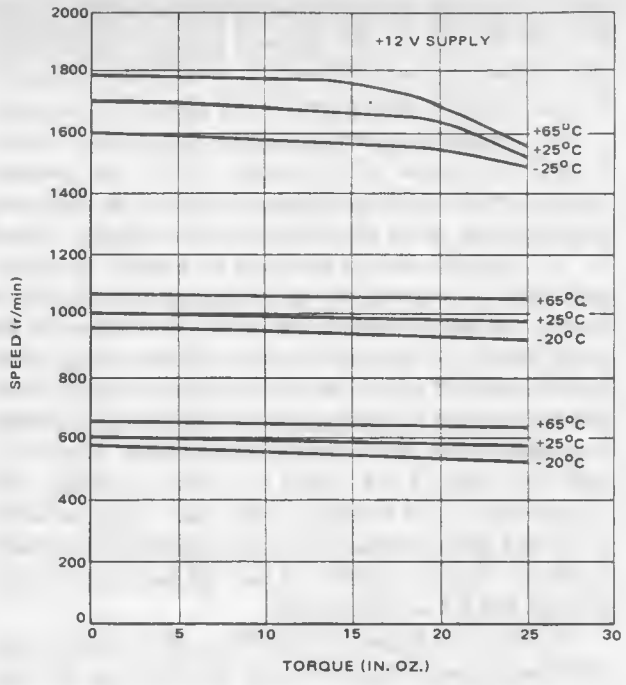

FIGURE 46 – Effect of Different Supply Voltages on Speed Control Circuit with Optical Feedback

Recall that the GaAs LED is 90% efficient with the MRD series, therefore, the equivalent output power of the LED is

$$P_E = (1.5mW)\,(0.9) = 1.35mW. \qquad (46)$$

From the MRD300 data sheet, S_{RECO} is found to be about 0.55 $mA/mW/cm^2$ minimum at H = 1.0mW/cm^2. This will cause a photo-current of

$$I_C = 0.55\ mA \qquad (47)$$

to flow. Thus for H = 1.0 mW/cm^2 Q3 should saturate. Converting Φ from degrees to radians, and recalling equation 34, we obtain

$$d^2 = \frac{4P_E}{H\pi\Phi^2}\ cm^2 \qquad (48)$$

or

$$d = 3.75\ cm \qquad (49)$$

Therefore, if the LED's are axially aligned with the MRD300 at a distance within 3.75 cm, saturation of Q3 is assured.

All four of these circuits can be used as the sensing part of a two-input static switch.

Phototachometer Motor Speed Control – To improve a motor's speed-torque characteristics, the circuit shown in Figure 44 can be used. This circuit illustrates a dc-motor speed control using an optical pick-off to complete the closed-loop system.

The motor armature is painted with alternate black and white stripes. A total of twenty stripes was used for the circuit shown. A fiber-optic bundle transmits light from a 12-volt lamp to the armature, and reflected light from the armature to the input of Q1, an MRD300 phototransistor. The light transmitted from bulb to armature to phototransistor is chopped at a frequency determined by the speed of the motor.

The output of the phototransistor is fed into a pulse-shaping circuit, and then into a tachometer circuit whose dc output is proportional to the input frequency. The output of the tachometer is fed to Q4, a junction field effect transistor. The JFET provides a high input impedance to minimize loading on the tachometer circuit, and a reasonably low output impedance to drive the differential amplifier. In addition, it acts as a level shifter to ensure that there is sufficient output to bias the differential amplifier when the tachometer output is zero. The diode in series with the source lead of the FET is used for temperature compensation.

The differential amplifier compares the fixed-speed-adjust voltage from R13 to the output of the tachometer level shifter and generates an output voltage that is proportional to the difference, or error, between the two. Capacitor C3 is used to prevent motorspeed overshoot when the speed-adjustment potentiometer is changed rapidly.

The T network (R15, R16, and C4) and zener diode D4 are used to reduce supply voltage variations to the pulse shaper, tachometer, level shifter, and comparator circuits.

The output of the comparator is amplified and fed into a pulse-width modulator. The output of the modulator is then fed into a Darlington circuit consisting of Q11 and Q12, which drives the motor.

The feedback for this circuit is derived from a direct measurement of the armature speed of the motor. This permits the speed of the motor to be well regulated as shown in Figure 45. An alternate method of temperature compensating the circuit can be accomplished by removing diode D3 and adding diodes in series with R9. Two or more diodes will probably be necessary for best temperature compensation, but one may yield satisfactory results.

Figure 46 shows the results of variations in the power supply voltage. The effects at lower supply voltages are greater since the pulse width reaches 100% and cannot be increased further to provide additional average motor voltage required by the load.

Optically Coupled Pulse Stretcher – The circuit shown in Figure 47 is used to stretch the width of an input pulse. Isolation is provided between the input and output pulses by using a phototransistor for the coupling element. The input pulse drives Q1, which in turn drives the light-emitting diode. The radiated pulse from the LED is coincident with the input pulse.

Phototransistor Q2 is used to prevent reset timing action in the monostable multivibrator consisting of Q3 and Q4. Transistor Q4 is normally on. When a light pulse appears, Q2 pulls base current away from Q4 and the collector voltage of Q4 rises. Regenerative action shuts Q4 fully off and turns Q3 fully on. Diode D1 clamps the negative voltage at the base of Q4 so that zener action is prevented in either the base-emitter of Q4 or the V_{ECO} mode of Q2.

When the light pulse is removed, the voltage at the base of Q4 begins to rise as the timing capacitor charges up. When this voltage reaches the turn on value for Q4, regenerative action causes Q4 to come full on while Q3 shuts off. The amount of pulse stretch is a function of the time constant of R5 and C1.

Figure 48 shows waveform variations within the pulse stretcher. When the input pulse turns the LED on, the output voltage rises to V_{CC}. The voltage transition at the collector of Q3 causes the base of Q4 to swing negative to the clamping voltage of D1. This voltage charges positively until sufficient bias is provided to the phototransistor Q2. The phototransistor holds in saturation until the LED shuts off with the turn off of the input pulse. The phototransistor shuts off and C begins to charge. When the base voltage of Q4 reaches about 0.5 volts, Q4 turns on fast and the output voltage goes low. For the circuit values in Figure 47, the pulse was stretched about 55 ms.

The separation distance between the LED and the phototransistor will again be a function of the putput power of the LED and the sensitivity of the phototransistor. This separation distance can be determined as was done for the optical logic drivers previously.

PAPER TAPE OR CARD READER

One very popular application for phototransistors is in the detection of punched, coded information on paper tape or cards. Since the density of punched information with regard to space is quite high, a requirement exists for transistor packaging to match such high density. This requirement is met in a series of Motorola photodetectors. The MRD100 and MRD150 are offered in the economical plastic Micro-T package, while the MRD200, MRD210, MRD250 and MRD600 offer a broad range of characteristics in the popular ceramic-metallic "pill" package. With the exception of the three-lead MRD100, all these devices are offered as two-lead (open-base) detectors.

The advantages offered by a phototransistor tape reader are quite obvious. The elimination of metallic brush contacts affords a significant increase in reliability and mean time between failure. A photoelectric system is totally non-contacting in nature, and offers potential

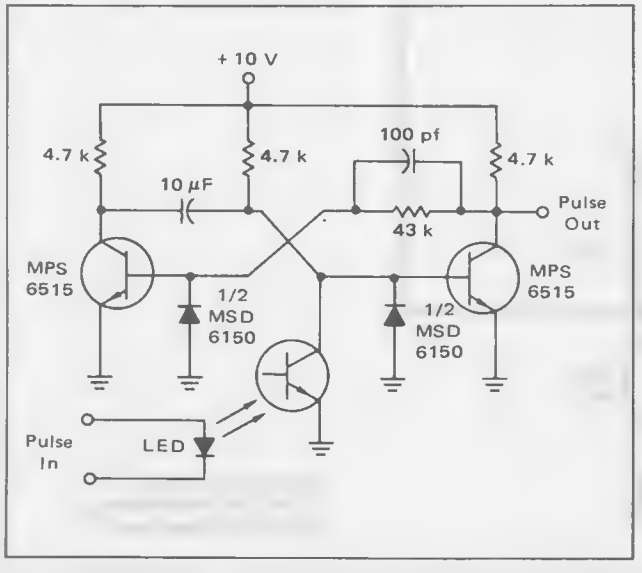

FIGURE 47 – Optically Driven Pulse Stretcher

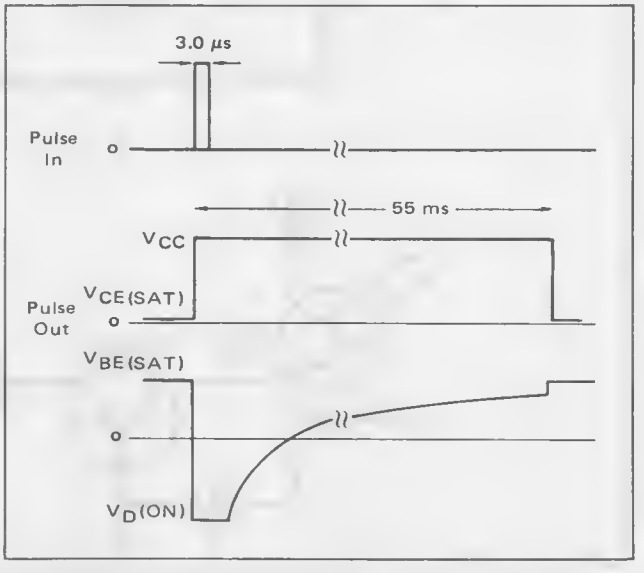

FIGURE 48 – Voltage Waveforms in the Pulse Stretcher

operating speed limited by the speed at which paper tape and cards can be transported without tearing. This speed capability is a result of mating a phototransistor with the previously discussed speed-up circuit to maintain a usable sensitivity-speed product.

The application of this circuit to a paper tape reader is shown in Figure 49. As shown, the circuit is designed for use with RTL logic.

Channel six of the tape serves as a clock input for the logic circuitry. A hole in the tape will cause the corresponding output line (for example the collector of Q3 for channel one) to go low. While the line is in the low state, the output of Q18 will be driven low by the passage of light through the trigger.

This will result in a "1" pulse, coincident with the trigger, at the corresponding gate output. This output pulse can now be used in any logic scheme compatible with RTL.

A critical factor in this system is the kind of paper used. Since the lamp is operated at very reduced voltage, its output is well into the infrared. The transmittance of paper tape to near-infrared is a function of the paper color. In the circuit of Figure 50, blue paper was used. This is a worst-case operation since blue was found to possess the highest transmittance. Greenish-yellow tape was found to have about 1/3 less transmittance and would give a more desirable light-dark ratio.

The same basic system can be used for a punched-card reader. The light-dark ratio is improved since the card is generally thicker and has a resultant lower IR transmittance.

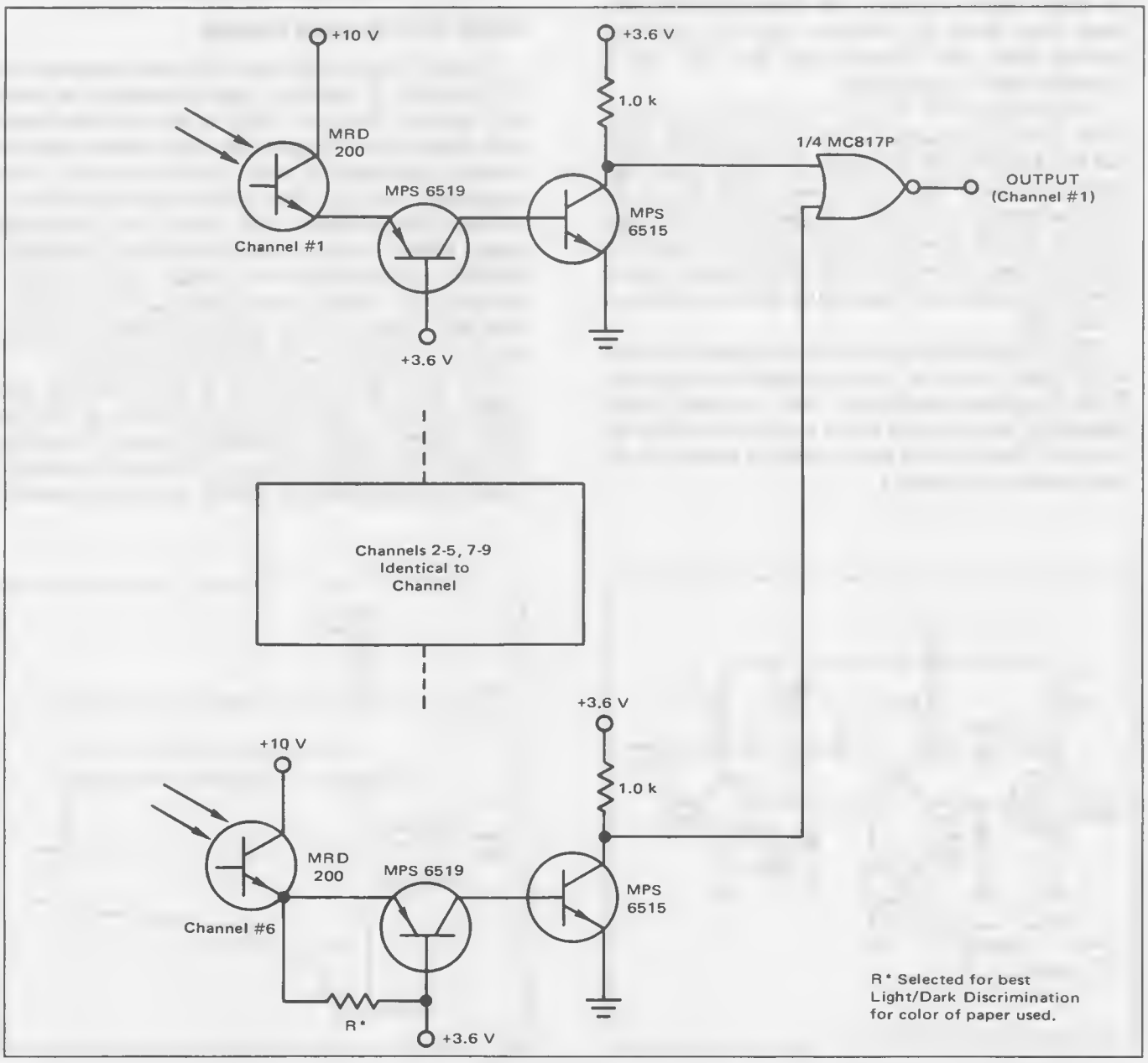

FIGURE 49 – Read Circuitry of Optical Paper Tape Reader

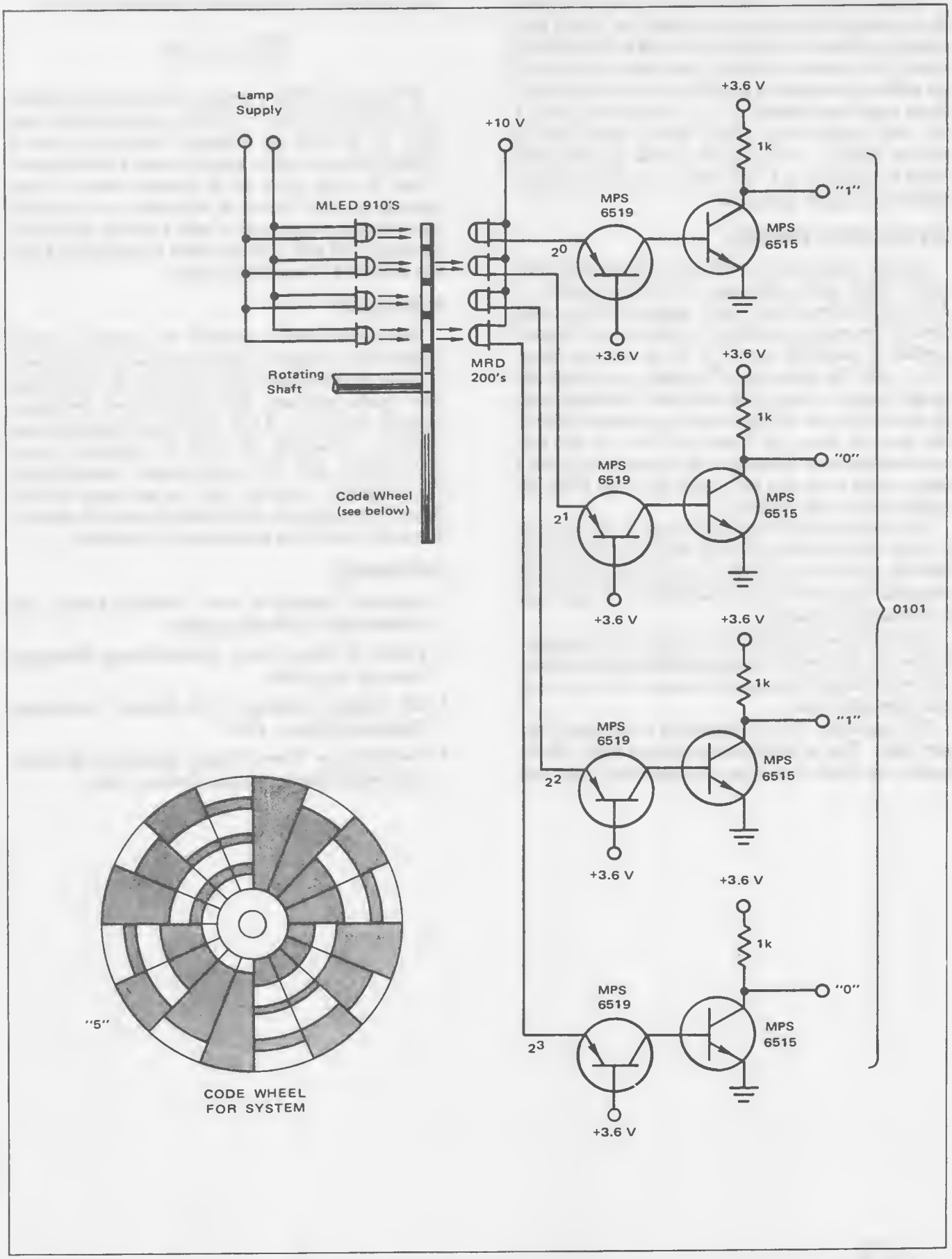

FIGURE 50 – Electro-Optical Shaft Encoder

A slight modification would allow the use of the circuit for automatic high-speed paper grading. The optical path would be reflective with the paper serving as the reflecting surface. The presence of a black pencil mark would reduce the reflection, resulting in an effective no input condition. If the same logic scheme as that in Figure 49 is used, a "0" will appear at the output when a pencil mark is scanned during a clock interval. In this case, the clock would be supplied as a "0" pulse at a rate functionally related to the paper scan speed.

OPTICAL SHAFT ENCODER

Another application in which the use of phototransistors offers certain advantages is the shaft encoder. A shaft encoder presents an output, usually in binary coded form, of the angular position of a shaft or other rotating member. A simplified version of this is shown in Figure 50. A code disc consisting of alternate transparent and opaque sections rotates with the shaft. Phototransistors are mounted in line with light sources on opposite sides of the disc. As shown in Figure 50, two of the four phototransistors are illuminated. If the devices represent a binary coded word with the outside bit as the 2^0 bit, the resultant data word is 0101 or 5.

The control system would now recognize that the shaft is in the fifth of sixteen positions. If a command code has called for position 12, or 1100, a comparator circuit would present an output which in turn would drive the shaft until it is in the proper position.

There are many applications for an optical shaft encoder. Typical are fire-control systems, tracking-radar systems, and automatic-process-control systems, such as a computer-controlled lathe.

The resolution of such a system is a function of the word size. That is, the four-bit system of Figure 50 can position the shaft to any one of 16 positions. This will place the shaft to a position with a maximum error of

$$\pm\frac{360}{16(2)} = \pm\ 11.25^\circ$$

By going to a five-bit system, 32 positions are available with an error of ± 5.625°. A high resolution system may use a 16 bit word for a position resolution of one in 65,536, with a maximum error of about ± 0.165 minutes of arc. A linear array of 16 phototransistors is quite practical, in either discrete or monolithic form, however, the remaining components of such a system, particularly the motor and gear train may limit the resolution below that afforded by the optical system.

CONCLUSION

The phototransistor provides the circuit or system designer with a unique component for use in dc and linear or digital time-varying applications. Use of a phototransistor yields extremely high electrical and mechanical isolation. The proper design of an electro-optical system requires a knowledge of both the radiation source characteristics and the phototransistor characteristics. This knowledge, coupled with an adequately defined distance and geometric relationship, enables the designer to properly predict the performance of his designs.

REFERENCES

1. Motorola Application Note AN-440, *Theory and Characteristics of Phototransistors.*
2. Francis W. Sears, *Optics,* Addison-Wesley Publishing Company, Inc., 1948.
3. *IES Lighting Handbook,* 3rd Edition, Illuminating Engineering Society, 1959.
4. *Semiconductor Power Circuits Handbook,* Motorola, Inc., Semiconductor Products Division, 1968.

MOTOROLA Semiconductor Products Inc.

Printed in Switzerland

AN 508